

IN SITU BIOFILM FORMATION AND BACTERIAL DEATH MONITORING USING
SURFACE-ENHANCED RAMAN SCATTERING

by
Esen Efeođlu

Submitted to the Institute of Graduate Studies in
Science and Engineering in partial fulfillment of
the requirements for the degree of
Master of Science
in
Biotechnology

Yeditepe University
2013

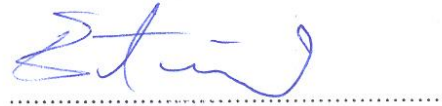
IN SITU BIOFILM FORMATION AND BACTERIAL DEATH MONITORING USING
SURFACE-ENHANCED RAMAN SCATTERING

APPROVED BY:

Prof. Dr. Mustafa ÇULHA
(Supervisor)



Prof. Dr. Ertuğrul KILIÇ



Asst. Prof. Andrew HARVEY



DATE OF APPROVAL: / /

ACKNOWLEDGEMENTS

Foremost, I would like to express my deep gratitude to my advisor, Prof. Mustafa ulha, for his support, patience, guidance, and invaluable advice throughout my Master education.

I would like to express my great appreciation to Yeditepe University Nanobiotechnology Group Members for their support during my thesis. I'm grateful to my friends Sercan Keskin and Ali Yasin Sonay for their help and stimulating discussions during my Master education. I would like to thank Zehra Yılmaz for taking SEM images. I also would like to thank Mehmet Kahraman, Sinan Sabuncu, Mine Altunbek, Seda Keleştemur and Selda Göktaş, Manolya Hatipođlu, Aslı Baysal, Şaban Kalay for their help and good advice. I would like to thank Assist. Prof. Kaan Keçeci for his help during my Master education.

I also would like to thank Prof. Ertuđrul Kılıç and Asst. Prof. Andrew Harvey for their help with my thesis. I want to express my gratitude to The Scientific and Technological Council of Turkey (TUBITAK) and Yeditepe University for financial support during my master education (Project No: 109T941). I also thank Prof. Dr. Fikrettin Şahin for providing the microorganisms used in the study.

Finally, I would like to express my deepest gratitude to my parents Öner Efeođlu and Zühal Efeođlu for their endless love, patience, and their confidence in me. I am also thankful to the other members of my family, Eren Soyaltın, Utku Soyaltın and Deniz Soyaltın for making my life more pleasurable.

I would also like to thank my friends especially Gamze Melis Başer, Nermin Başak Şentürk, Nihan Kılınç, Nur Ekimci, Sinem Ethemöđlu, Merve Erdem, Ayca Zeynep İlder, Serhat Büyüktanır and Sabiha Demirci for their continuous support and understanding whenever I needed.

ABSTRACT

***IN SITU* BIOFILM FORMATION AND BACTERIAL DEATH MONITORING USING SURFACE-ENHANCED RAMAN SCATTERING**

Surface-enhanced Raman scattering (SERS) is a powerful technique for characterization of biological molecules and molecular structures due to the fingerprinting property, very narrow spectral bandwidth, and easy sample preparation. In SERS, Raman scattering can be enhanced up to 10^{14} times by bringing the molecule or molecular structure of interest close to or in contact with nanostructured noble metals such as gold and silver. SERS can be used for the characterization and identification of components of complex biochemical systems such as bacteria and biofilm. In this thesis, characterization and identification of biofilm components were investigated using SERS. The core AgNP- shell chitosan layer type structure was prepared by coating the AgNPs with a layer of chitosan (c-AgNPs) and they were used as a SERS substrate for biofilm formation and bacterial death monitoring. Due to absorptive property of chitosan, biomaterials that were produced by bacteria can penetrate into shell without saturating the metal surface due to the selective interaction of biofilm components with the AgNPs. The feasibility of *in situ* monitoring of molecular changes during the bacterial death was also demonstrated. It was found that SERS spectra could provide significant information about the morphologic changes on the bacterial cell wall and released molecular structures such as DNA/RNA bases during the decomposition of bacteria. It was also found that the band at 678 cm^{-1} could be used for monitoring bacterial death.

ÖZET

YÜZEYDE ZENGİNLEŞTİRİLMİŞ RAMAN SAÇILMASI İLE BİYOFİLM OLUŞUMU VE BAKTERİ ÖLÜMÜNÜN YERİNDE İZLENMESİ

Yüzeyde zenginleştirilmiş Raman saçılması (YZRS) parmak izi özelliği, oldukça dar spektral band aralığı ve kolay örnek hazırlanması sebebiyle biyolojik moleküllerin ve moleküler yapıların karakterizasyonu için güçlü bir tekniktir. YZRS’de, Raman saçılması, ilgili molekül ya da moleküler yapıların nanoyapılar halindeki altın ve gümüş gibi soymetaller ile yakın veya temas durumuna getirilerek 10^{14} kat zenginleştirilebilir. YZRS, bakteri ya da biyofilm gibi kompleks biyokimyasal sistemlerin bileşenlerinin tanımlanması ve karakterizasyonu için kullanılabilir. Bu tezde, biyofilm bileşenlerinin tanımlanması ve karakterizasyonu YZRS kullanılarak araştırıldı. Çekirdek AgNP-kabuk kitosan tabaka şeklinde yapı, AgNP’ların kitosan tabaka ile kaplanmasıyla hazırlandı ve bu yapılar biyofilm oluşumu ve bakteri ölümünün gözlemlenmesi için YZRS substratı olarak kullanıldı. Kitosanın absorptif özelliğinden dolayı, bakteri tarafından üretilen biyomateryaller biyofilm bileşenlerinin AgNP ile seçici etkileşimlerinden dolayı metal yüzeyini doyurmadan kabuk içerisine girebilir. Ayrıca bakteri ölümü sırasındaki moleküler değişikliklerin yerinde izlenebilirliği gösterildi. YZRS’nin bakteri hücre duvarındaki morfolojik değişimler ve bakteri dekompozisyonu sırasında salınan DNA/RNA gibi moleküler yapılar hakkında önemli bilgi sağlayabildiği bulunmuştur. Ayrıca, 678 cm^{-1} deki bandın bakterinin ölümünün izlenmesinde kullanılabileceği bulunmuştur.

TABLE OF CONTENTS

ACKNOWLEDGEMENTS.....	iii
ABSTRACT.....	iv
ÖZET	v
TABLE OF CONTENTS.....	vi
LIST OF FIGURES	viii
LIST OF TABLES.....	x
LIST OF SYMBOLS / ABBREVIATIONS.....	xi
1. INTRODUCTION	1
2. THEORETICAL BACKGROUND.....	4
2.1. MICROORGANISM	4
2.1.1. Bacterial Growth.....	5
2.2. BIOFILM	7
2.3. RAMAN SCATTERING AND SURFACE ENHANCED RAMAN SCATTERING.....	7
2.3.1. Theory of Raman Spectroscopy	7
2.3.2. Plasmonics and Plasmonic Structures as SERS substrate.....	10
2.3.3. Modification of SERS Substrates	12
2.3.4. Detection and Identification of Microorganisms	13
3. MATERIALS	15
2.1. CHEMICALS.....	15
4. METHOD	16
4.1. PREPARATION OF BACTERIA SAMPLES	16
4.2. PREPARATION OF COLLOIDAL SILVER NANOPARTICLES	16
4.3. PREPARATION OF CHITOSAN COATED AgNPs AND BACTERIAL SAMPLES FOR SERS MEASUREMENT.....	17
4.4. MONITORING DEATH OF <i>E. COLI</i> EXPOSED TO AN ANTIBIOTIC.....	18
4.5. CONSTRUCTION OF GROWTH CURVE OF <i>E. COLI</i>	19
4.6. ANTIBIOTIC SUSCEPTIBILITY OF <i>E. COLI</i>	19
4.6.1. Disc Diffusion.....	19

4.6.2. Effect of Antibiotic in the Growth of <i>E.coli</i>	19
4.7. RAMAN MICROSCOPY SYSTEM.....	19
4.8. SEM MEASUREMENT	20
4.9. TEM MEASUREMENT.....	20
4.10. ZETA SIZE (DLS and ZETA POTENTIAL ANALYSIS).....	20
5. RESULTS AND DISCUSSION	21
5.1. IN-SITU MONITORING OF BIOFILM FORMATION BY USING SERS....	21
5.2. OBSERVATION OF BACTERIAL DEATH FROM SERS SPECTRA.....	32
6. CONCLUSION AND RECOMMENDATIONS	39
6.1. CONCLUSION.....	39
6.2. RECOMMENDATIONS.....	40
7. REFERENCES	41

LIST OF FIGURES

Figure 2.1. Several categories of microorganisms: a. algae, b. protozoa, c. virus , d. fungi, and e. bacteria	4
Figure 2.2. General growth curve for bacteria.....	6
Figure 2.3. Rayleigh scattering-Raman scattering.....	8
Figure 2.4. Schematic illustration of surface plasmons that localized around the nanoparticle	11
Figure 2.5. Simulation of surface plasmons around the nanoparticles and the change of ‘SP’ depends on shape of nanoparticles	11
Figure 2.6. SEM image of AgNPs obtained by citrate reduction method	12
Figure 2.7. Structure of Chitosan.....	13
Figure 4.1. Preparation of bacterial samples for SERS acquisitions	17
Figure 4.2. Preparation of bacterial samples in the presence of ampicillin for SERS acquisition	18
Figure 5.1. a. SEM image, b. TEM image, c. UV/Vis spectra and d. dynamic light scattering (DLS) spectra of AgNPs before and after coating.....	22
Figure 5.2. SERS spectra of c-AgNPs, after their addition onto nutrient agar (NA) and tryptic soy agar (TSA).....	23
Figure 5.3. Reproducibility of SERS spectra of a. <i>E. coli</i> and b. <i>S. cohnii</i> . Inset	

images are white-light image of c-AgNP aggregates on culture plate.....	24
Figure 5.4. SERS spectra of <i>E. coli</i> biofilm during incubation time from 3 to 48 h. Each spectrum is the average of five spectra obtained from the same droplet area on the culture plate	27
Figure 5.5. SERS spectra of nucleic acid bases, A, C, G and T. Each spectrum is the average of five spectra acquired from each sample	28
Figure 5.6. SERS spectra of <i>S. cohnii</i> biofilm during incubation time from 3 to 48 h. Each spectrum is the average of five spectra obtained from the same droplet area on the culture plate	31
Figure 5.7. The growth profile for <i>E.coli</i> at OD ₅₅₀	33
Figure 5.8. The growth profile of <i>E.coli</i> in presence of 2.0 mg/mL and 0.2 mg/mL ampicillin.....	34
Figure 5.9 Reproducibility of SERS spectra for <i>E. coli</i> in the presence of a. 2.0 mg/mL and b. 0.2 mg/mL ampicillin at the end of incubation period for both bacteria	35
Figure 5.10 SERS spectra obtained during the death of <i>E. coli</i> with the addition of a. 0.2 mg/mL and b. 2.0 mg/mL ampicillin at different times	37

LIST OF TABLES

Table 5.1. Tentative band assignments on the SERS spectra acquired from biofilm using c-AgNPs	26
---	----

LIST OF SYMBOLS / ABBREVIATIONS

AgNPs	Silver nanoparticles
c-AgNPs	Chitosan coated AgNPs
CLSM	Confocal laser scanning microscopy
CT	Charge transfer enhancement
DLS	Dynamic light scattering
DNA	Deoxyribonucleic acid
EM	Electromagnetic enhancement theory
EPS	Extracellular polymeric substance
FTIR	Fourier transformed infrared spectroscopy
h	Hour
IR	Infrared
kV	Kilovolts
log phase	Logarithmic phase
LSP	Localized surface plasmons
LSPR	Localized surface Plasmon resonance
mg	Milligram
MIC	Minimum inhibition concentration
MIDI	Microbial Identification System
MS	Mass spectroscopy
mW	Miliwatt
MW	Molecular weight
NA	Nutrient agar
NB	Nutrient broth
nm	Nanometre
OCT	Optical coherence tomography
OD	Optical density
PBS	Phosphate Buffered Saline
PSP	Propagating surface plasmons
RNA	Ribonucleic acid
s	Second

SEM	Scanning electron microscopy
SERS	Surface-enhanced Raman scattering
SPR	Surface Plasmon resonance
SPs	Surface Plasmons
TEM	Transmission electron microscopy
TEM	Transmission electron microscopy
TSA	Tryptic soy agar
UV/Vis	Ultraviolet/Visible

1. INTRODUCTION

Microorganisms are too small to be seen with naked eye. After adhering onto surfaces, extracellular polymeric substance (EPS) production occurs as a result of vital activities of microorganisms. The biofilm formation can take place on solid surfaces or aqueous environments under several conditions [1]. The biofilm structure contains both microorganism and EPS that primarily consists of polysaccharides, genetic materials, proteins, lipids and humic-like substances, which are mixtures of degraded and transformed products of bioorganic materials [2, 3]. Not only the identification of the components but also the monitoring of the molecular changes in a biofilm composition may clarify the mode of interaction of microorganisms with their environment during their growth. Therefore, a better understanding of biofilm composition and changes in composition during the growth of microorganisms is critically important.

Most of the previous studies for biofilm characterization were based on visualization of EPS, after a staining step, by confocal laser scanning microscopy (CLSM) [4-8] and optical coherence tomography (OCT) [9]. Not only the complex nature of biofilm but also difficulty in protocol development with CLSM and OCT limits their use [10-12]. Transmission electron microscopy (TEM) can also be used for biofilm characterization [13, 14]. Although TEM studies provide detailed information about biofilms, sample preparation may alter the integrity of a biofilm and decrease the reliability of the results. Vibrational spectroscopic techniques such as IR and Raman spectroscopies were also used for the characterization of biofilms. Fourier transform infrared spectroscopy (FTIR) can provide valuable information about the biochemical composition of biofilms [15]. However, it has a limited spatial resolution and water in samples can cause a significant problem. Raman spectroscopy has also been used for characterization of biofilms [16, 17]. Raman spectroscopy has been proven to be a powerful technique to study a variety of biological and non-biological molecules and molecular structures [18, 19]. The major advantages of Raman spectroscopy are easy sample preparation, limited influence from water that is a part of biological samples, and narrow spectral bandwidths that can be used to understand the composition of a sample. With the recent developments in instrumentation, it can now be used to obtain chemical information from a given location

on a sample with a high spatial resolution (down to a few micrometers) [20]. Although easy sample preparation makes its use more advantageous, inherently weak scattering is an important drawback of the technique. The high laser powers and increased exposure times can increase the amount of scattered light but the sample can be damaged under such conditions. With the discovery of surface-enhanced Raman scattering (SERS), it is now possible to enhance the Raman scattering easily up to 10^8 times by placing the molecule of interest in the close vicinity of a nanostructured surface or colloidal nanoparticles of a noble metals such as gold and silver [21-25].

SERS has been used for *in situ* measurements of signaling molecules in bacteria quorum sensing and biofilm characterization [11, 12, 26, 27]. These early studies demonstrated the power of the technique to use for biofilm formation monitoring and characterization. In all of these reports, the colloidal AgNPs synthesized with a reducing agent such as sodium citrate, borohydride, and hydroxylamine hydrochloride were used as substrates. As different from the previous studies, we used citrate reduced AgNPs coated with chitosan, which not only prevents dissolution of AgNPs but also acts as a selective barrier in very complex biological environment.

Chitosan is a natural polymer that obtained by deacetylation of chitin. It is a linear polymer composed of D-glucosamine units linked by β -(1 \rightarrow 4) bonds. Chitosan intrinsically exhibits unique properties such as biocompatibility and biodegradability. Due to these properties, chitosan has widely used in medicine and industrial applications. In addition, since chitosan carries $-\text{NH}_2$ groups in its structure, it carries positive charge at around physiological conditions and interacts with highly negatively charged species such as DNA and RNA. Therefore, the use of chitosan nanoparticles for gene and RNA delivery was reported [28, 29]. Its use in preparation of Raman-active probes with good biocompatibility was also reported [30, 31].

In this study, we investigated the use of SERS for the changes in the biofilm composition *in situ* using AgNPs coated with a chitosan shell (c-AgNPs) as substrates. The core-shell particles are directly spotted on the bacterial culture plate and the SERS spectra from the spotted location were acquired. First, we assessed the reproducibility of the SERS spectra resulted from such sampling approach. Then, the SERS spectra were acquired from the

biofilms during the growth and evaluated against the molecular changes in the biofilm. This study differs from the previous reports with the use of c-AgNPs. The presence of polymeric shell not only acts as a selective barrier preventing the quench of surface plasmons but also prevents the dissolution of AgNPs. Moreover, in the second part of the thesis, we investigated the spectral changes during the death of bacteria in the presence of ampicillin antibiotic. The effect of different antibiotic concentrations on the morphology of bacterial cell wall was monitored. The components released from the bacteria cells during bacterial death were used to determine the bacterial death.

2. THEORETICAL BACKGROUND

2.1. MICROORGANISM

The word ‘microorganism’ comes from Greek word micro, which indicates the size. As a small life form of organisms, microorganisms include the viruses, bacteria, fungi, protozoa and algae (Figure 2.1). Although microorganisms are the earliest life forms in our world, the recognition of them lies just a few centuries ago due to the lack of imaging technologies. With the invention of microscopes, the existence of a very rich microbial world has been realized [32].

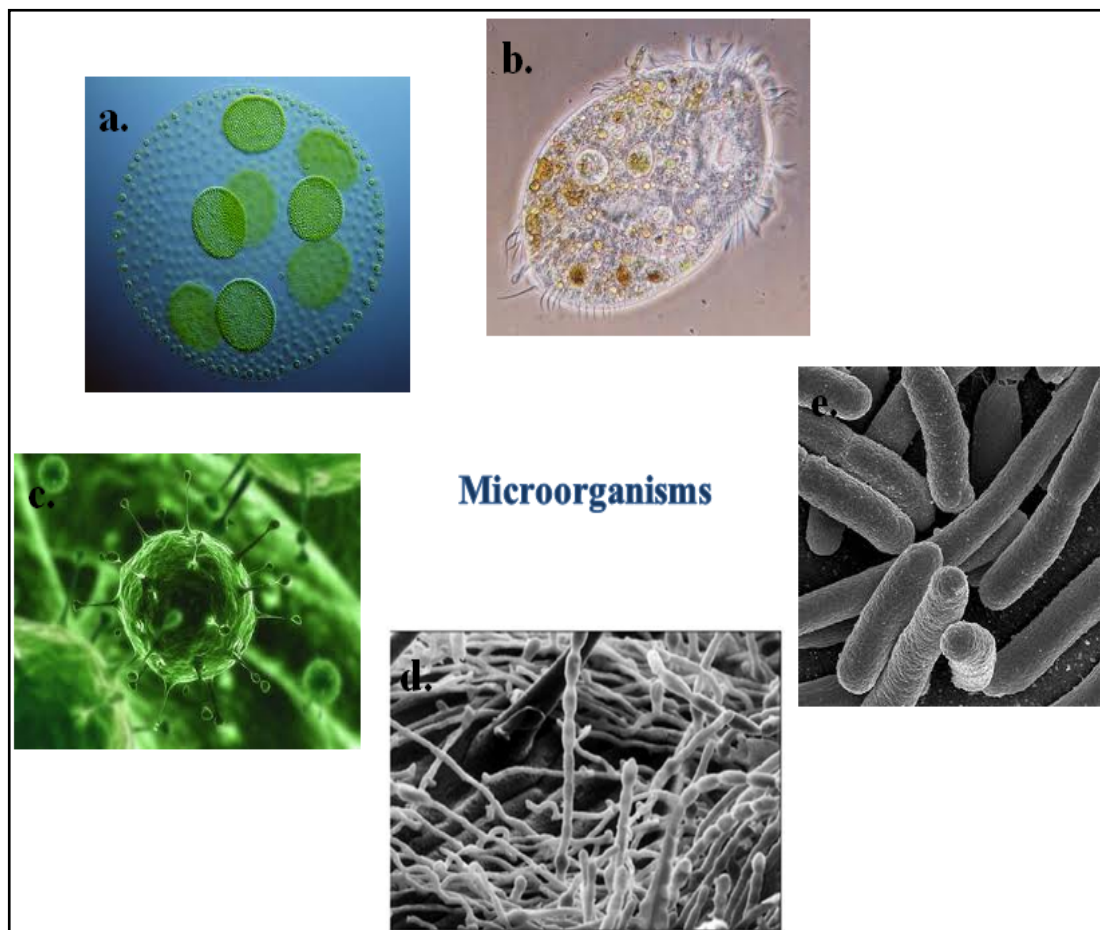


Figure 2.1. Several categories of microorganisms: a. algae, b. protozoa, c. virus, d. fungi , and e. bacteria

Although there are some exceptions as molds and many algae, also known as multicellular and eukaryotic, most of the microorganisms are single-celled. Prokaryotes are the most abundant and diverse organisms on Earth. Among microorganisms, bacteria are known as the least complex structures. Because of their diversity and metabolic activity, they can be found everywhere in *biosphere*. They are in our foods, water that we drink, clothes, air, etc. They do not contain a membrane-bound nucleus and any other organelles in their structures. Metabolic activities take place in cytoplasm. The genetic material is found in suspended portion of the cytoplasm that is called as nucleoid. They are divided into two groups as bacteria and archaeobacteria. Except a few groups, prokaryotic cells are surrounded by cell wall, which is composed of peptidoglycan. Peptidoglycan structure made up of glycan strands linked by short peptides. Each strand consists of acetylglucosamine (GlcNAc), N-acetylmuramic acid (MurNAc) linked by β -(1 \rightarrow 4) bands [33]. This layer provides support and resistance to osmotic changes. The thickness of peptidoglycan layer changes according to gram type of bacteria. It shows a similar function to eukaryotic cell wall, however it has different chemical composition. In bacteria, ribosomes where all protein synthesis takes place are found in cytoplasm. Actually, their plasma membrane is composed of lipid bilayer as eukaryotes however, sterols are rarely found in bacteria structure [34].

2.1.1. Bacterial Growth

All microorganisms require suitable physical and chemical conditions, enough nutrition and minimum competition for their growth. Understanding and controlling of growth requirements of microorganisms prevent unwanted growth and help achievement of maximum product yield. These parameters can be controlled by the manipulation of some essential factors such as water and energy source, essential elements like C, H, O₂ and N₂ and growth factors. Although chemical conditions are important, physical conditions have also important role in bacterial growth. Temperature, pH, O₂ and osmotic pressure are the most important environmental factors for proliferation. When all necessary conditions were provided, microorganisms started to metabolize and grow in size and number. Briefly, they tend to proliferate at the maximum rate. The growth of the bacteria can be used as advantageous. Harmful activities can be prevented and useful metabolic products can be used. Dynamics of bacterial growth can be monitored. Generally their growth

occurs in four phases; lag phase, logarithmic (log) phase, stationary phase and death phase, as seen in Figure 2.2. The lag phase is known as adjustment period for bacteria. When bacteria encounter the new environment, they tend to adapt rather than proliferate. During this period, bacteria need to synthesize enzymes and proteins to retrieve the previous environmental conditions. This phase can generally be short or absent according to metabolic activity of bacteria.

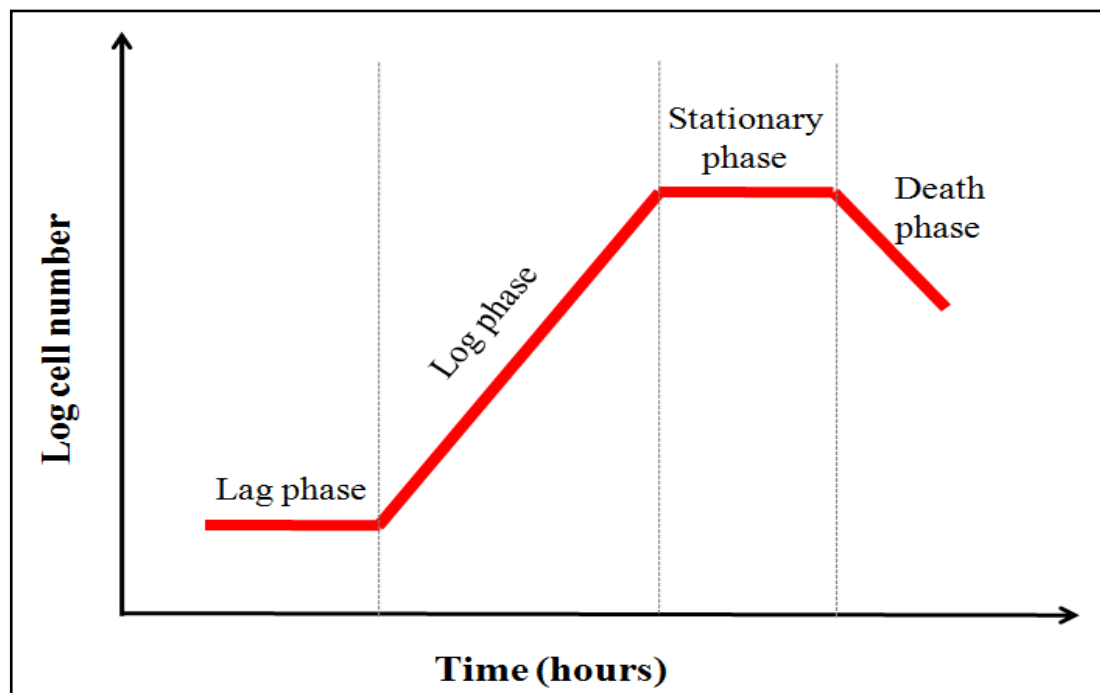


Figure 2.2. General growth curve for bacteria

After microorganisms adapted to environment, they begin to divide at their maximum rate. This means that DNA synthesis occurs at maximum rate. Although protein synthesis proceeds, synthesized DNA/protein ratio increase. During the log phase, bacteria become more sensitive to any inhibitory or antibiotics because of their high metabolic activity. In the stationary phase, there is no change in the population size. The bacteria that produced become equivalent to the bacteria, which are dying. Secondary metabolites are synthesized during stationary phase. If conditions do not change during stationary phase, bacteria begin to lose their integrity and go death phase [34].

2.2. BIOFILM

Microorganisms produce extracellular polymeric substances (EPS) as a result of vital metabolic activities after adhering onto surfaces. The structure that contains both microorganism and EPS is called as biofilm. EPS matrix is composed of genetic materials, proteins, lipids, polysaccharides and humic-like substances [1]. Extracellular polysaccharides were synthesized by most of the bacteria either as cell wall component or as extracellular secretions. The biofilm formation can occur under several conditions and different media such as solid surface or aqueous environments [2]. There are several factors that affect the formation of biofilm structure such as the composition of microbial community, nutrient availability, surface properties etc. [35]. Formation of biofilm structure has some advantages for microorganisms as protection from the environment and acquisition of new genetic traits. EPS component of biofilm provide a shelter for microorganisms. It also prevents the access of antimicrobial agents to the microorganisms. Water channels in biofilm structure provide a permeable barrier and circulatory system for microorganisms. Nutrients and metabolites change via the water channels and they remove toxic metabolites from the environment [36]. Biofilm provides an ideal environment for syntrophism among metabolically distinct microorganisms. Moreover, it constitutes an environment for horizontal gene transfer. Therefore, it provides evolution and genetic diversity.

2.3. RAMAN SCATTERING AND SURFACE ENHANCED RAMAN SCATTERING

2.3.1. Theory of Raman Spectroscopy

Spectroscopy is the study of the interaction between matter and light. The light is composed of photons, and when it interacts with matter, several processes such as absorption, transmission and scattering can take place. During this interaction, if the energy of photon (I_0) corresponds to the energy gap between the ground state and excited state of the molecule, photons (I) may be absorbed by the molecule and the molecule is excited to a higher energetic state. This type of change can be measured by absorption spectroscopy by using differences between I_0 and I [37].

Raman scattering is known as the inelastic collision of photons with molecules. The theory of scattering was experimentally demonstrated by Raman in 1928 [38]. Due to the inherently weak scattering compared to fluorescence, it requires a powerful light source and sensitive detector. If the photons scatter from molecules, these scattered photons can be collected at an angle of the incident light. In this type of interaction, photon carries out low energy. In this case, molecule excited to the virtual states between vibrational states and lower excited electronic states [38, 39]. Jablonski diagram was used for the quantum explanation of Raman scattering (Figure 2.3). Generally, the most of the scattered photons from molecules or atoms have equal frequency with the incident light and this phenomenon is called as Rayleigh scattering ($I_0=I$). On the other hand, Rayleigh scattering can change in a very small amount ($1/10^7$) as a gain or loss in vibrational energy, which correspond to the Stokes and Anti-stokes shift, respectively.

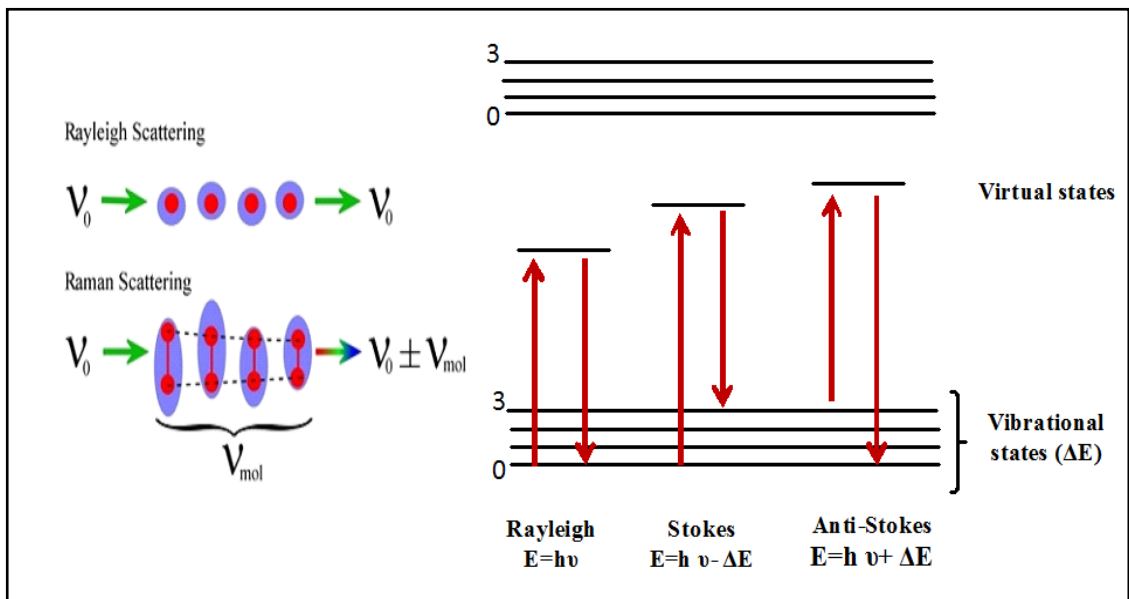


Figure 2.3. Rayleigh scattering-Raman scattering [40]

Stokes frequency can be defined with the equation; $\nu_0 - \nu_m$. When a photon (ν_0) is absorbed by Raman-active molecule at initial vibrational state, a part of the photon's energy transfer to the electrons of molecule and the molecule gains frequency (ν_m). As a result, the frequency of scattered light reduces. On the other hand, when a photon is absorbed at virtual states, excessive energy is released and molecule turns back to the

initial vibrational state with higher frequency of scattered light. Equation becomes $\nu_0 + \nu_m$ [39].

When light interacts with a molecule, it acts as a propagating oscillating dipole. It distorts the electron cloud around the nuclei and result in polarization of electrons and dipole moment formation in the molecule. During this interaction short-lived complex between light and electrons occur. This complex is not stable so light released as a scattering in a short time. Therefore, it is called as virtual states. On the other hand, electron cloud relaxes as a result of the interaction of light during Rayleigh scattering without any nuclear movement.

When light scattered from a molecule, it changes its conformation through changing the electron oscillation. For example, a molecule can rotate or vibrate due to different energy states that are gained from the incident light. In an atom or molecule, these vibrations arise from groups such as carbon chain and ring forms that linked by bonds with almost the same energy. The overall shape of molecule is determined by the number of peaks and energies of them. These bands are known as “*fingerprint bands*” and the pattern of them can give highly important information about the chemical structure of the molecule. Thus, Raman scattering can be used to identify a specific molecule *in situ* [41, 42].

Raman spectroscopy is a powerful technique to study variety of biological and non-biological molecules and molecular structures [19, 43]. The advantages of Raman spectroscopy can be given as easy sample preparation, limited interference from water, and very narrow spectral bandwidths allowing multiplex detection of components in a mixture. With the introduction of micro-Raman spectrometers it is now possible to obtain chemical information from a few micrometer size area on the sample [20]. The major disadvantage of the technique is the inherently weak signal. Increased laser power and exposure time can help to improve measurement but the sample can be decomposed under the laser light in such case. With the discovery that Raman scattering process can be enhanced by bring the molecule or molecular structure into close proximity of a nanostructured noble metal surface, which is called surface-enhanced Raman scattering (SERS), it is now possible to enhance the Raman scattering easily up to 10^8 times [21, 25].

SERS was firstly reported by Fleischman et al. and they have showed the effect of silver electrode roughness on the spectra of pyridine [44]. Since the first report of the technique, there have been several theories that were proposed to explain SERS. However, currently theories, which are used to explain SERS, can be divided into two groups as *Electromagnetic enhancement (EM)* and *Charge transfer enhancement (CT)* [22, 45-47]. In electromagnetic theory, enhancement occurs as a result of surface plasmons that occur around the nanoparticles. When the Raman scatterer interacts with plasmonic area (intense electromagnetic area), induced dipole moment and inelastic collision increase [48]. In charge transfer theory, enhancement occurs as a result of electrons' movement between metal and molecule. Briefly, higher oscillation of the electrons in metal induces the oscillation in the molecule and result in an enhancement on spectrum. However, it is known that, the effect of electromagnetic enhancement (10^{4-7}) is more than charge transfer enhancement ($10-10^2$) [47].

2.3.2. Plasmonics and Plasmonic Structures as SERS substrate

Plasmonics study interaction between metal and light [49-51]. It is related to localization and manipulation of electromagnetic waves beyond the diffraction limit and down to nanometer-length scale. Surface plasmons (SPs) are known as the coherent oscillation of conductive electrons on metal surface. Surface Plasmon resonance can be divided into two groups as propagating (PSP) and localized surface plasmons (LSP) [52, 53]. The electric field that depends on the light (E_0) applies a force on the electrons of the metal and drives them to oscillate. When the oscillation is in resonance with the light at a certain wavelength, it leads to a forceful oscillation on the surface electrons. This phenomenon is called as localized surface Plasmon resonance 'LSPR' (Figure 2.4). When resonant wavelength is absorbed on the metal surface, it causes a change on the vibration of electron cloud. This is called as Surface Plasmon Resonance 'SPR'.

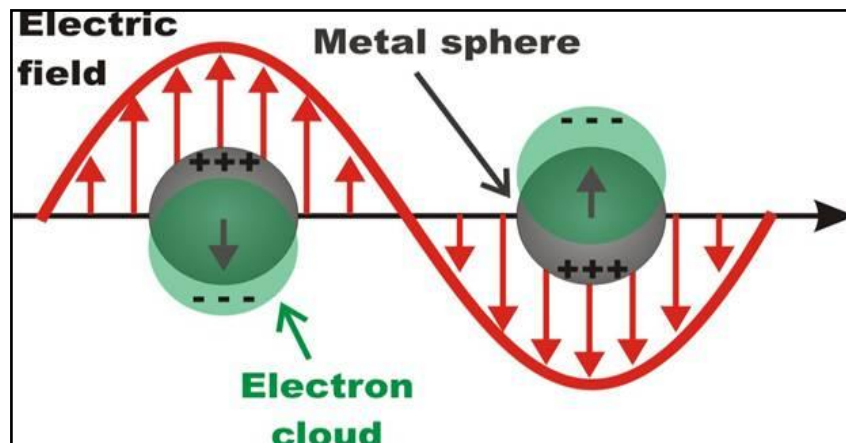


Figure 2.4. Schematic illustration of surface plasmons that localized around the nanoparticle [54]

The property of surface plasmons can change according to the type, shape, size, composition and dielectric environment of nanoparticles as seen in Figure 2.5.

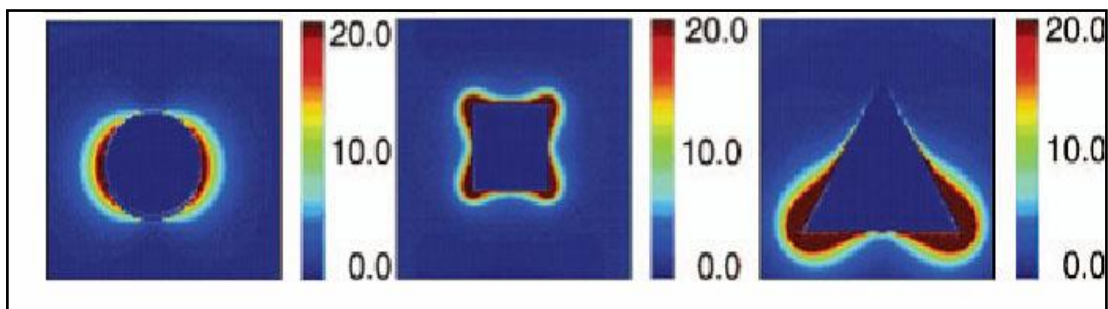


Figure 2.5. Simulation of surface plasmons around the nanoparticles and the change of 'SP' depends on shape of nanoparticles [55]

The application areas of these plasmonic nanostructures can be counted as optical spectroscopy in nano dimensions [56], SERS [57], SPR [53, 58] and LSPR [59]. These plasmonic structures can absorb or scatter the light and this absorption and scattering features of the material can be changed. Therefore, these plasmonic structures can be used in various fields such as biomedical imaging [60], biophysical studies [61], diagnosis [62] and cancer treatment [63, 64]. The type of SERS substrates can vary from colloidal particles to rationally designed nanostructures depending on the application. Especially, metallic nanoparticles such as Au, Ag, Cu, Li and Al support surface plasmons in

Ultraviolet/Visible (UV/Vis) and near-infrared regions. As a significantly important plasmonic material, silver nanoparticles (AgNPs) have gained importance due to their wide range to support light in the region of 300-1200 nm. Moreover, their extraordinary optical and electrical properties expand their use in various fields such as electronics, bio-labeling, catalysis and SERS. Although there are several methods to obtain AgNPs such as reduction with organic and inorganic agents [65, 66], ultrasound, UV light and Gamma rays [67], they can easily prepared by citrate reduction method. The synthesized AgNPs with citrate reduction carry negative surface charge due to presence of citrate ions in the solution. The only drawback of this technique is the uniformity of the generated AgNPs. As seen in Figure 2.6, they have several different sizes and shapes with an average size of 60 nm.

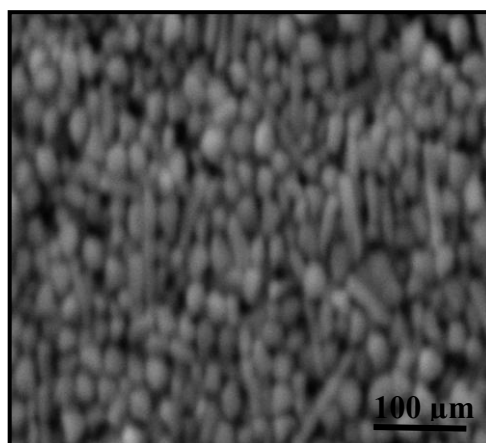


Figure 2.6. SEM image of AgNPs obtained by citrate reduction method

2.3.3. Modification of SERS Substrates

Metal nanoparticles can be modified with various molecules and polymers. In SERS experiments, coating of AgNPs with polymers such as pluronic and chitosan provide higher dispersion, long-term stability and it may help to increase the enhancement further [30, 68].

Surface plasmons are generally localized at the junctions and grooves of nanostructures. When two nanoparticles are brought together, surface plasmons coincide and enhancement is further improved. These areas are called as '*hot spots*' [30]. Polymer coating provides the formation of these hot spots resulting in maximum enhancement. Moreover, c-AgNPs

prevent dissolution of AgNPs, and also act as a selective barrier in very complex biological environment.

Chitosan is a biocompatible and biodegradable natural polymer derived from deacetylation of chitin (Figure 2.7). It is used in a wide range of applications and its use to coat the AgNPs to use in SERS has already been reported [28-31].

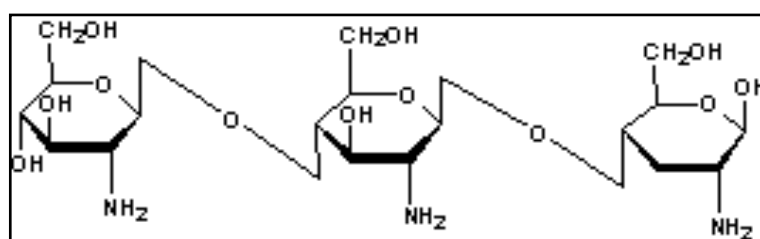


Figure 2.7. Structure of Chitosan

2.3.4. Detection and Identification of Microorganisms

The identification and characterization of microorganism is vital for the understanding their relations with environment and human health. The phenotypic tests, serological tests, cellular fatty acid profiles, protein profiling, nucleic acid probes, genomic and traditional methods based on eye examination and staining can be counted as methods to identify bacteria [69,70]. Although these techniques are very useful to identify bacteria, they require expensive instrumentation and trained personnel. In addition, they are time consuming. Therefore, researchers have used spectroscopic techniques and the use of spectroscopic techniques such as mass spectroscopy (MALDI, PyMS) [71-73], IR and Raman spectroscopy have been reported [74-76]. Among these techniques mass spectroscopy requires relatively high cost and trained personnel. IR and Raman spectroscopy can be more suitable due to easy sample preparation steps [77-79]. However, Raman is a promising technique because of its compatibility with water and water including samples such as biological samples. The use of Raman spectroscopy for biological samples such as bacteria and living cells has been demonstrated [78, 80, 81]. Insufficient signal of Raman scattering can be a drawback for biological samples due to the use of higher laser power and accumulation. The weak signal can be enhanced on the

surface of metal nanoparticles. With the appearance of SERS, it has started to be used for identification and detection of biological molecules and characterization of structures such as living cells and microorganisms [82, 83]. It provides fingerprint information due to narrow spectral bands in addition to water compatibility. In SERS studies that have been used for bacteria, Au and Ag nanoparticles were preferred. The feasibility of SERS for identification and classification of microorganisms have described [84-88], after Holt and Cotton [89] reported the use of SERS for photosynthetic bacterium. Moreover, cell wall and components have been studied by Efrima, Bronk and Zeiri et. al.. They showed the differences in the SERS spectra obtained from cell wall and from inside the cell. SERS for bacteria also have studied by Sengupta et al. and Laucks et al. [86-90]. In this study, colloidal nanoparticles were absorbed on the cell wall and different colloidal conditions such as size, aggregation was investigated. Jarvis et al. developed a different sample preparation and in the study, silver colloidal solution was mixed with bacteria solution and SERS spectra were taken dried samples [87, 91].

3. MATERIALS

3.1. CHEMICALS

Nutrient agar (NA), nutrient broth (NB), tryptic soy agar (TSA) and sodium citrate (99 per cent) were purchased from Merck. AgNO_3 (99.5 per cent) was purchased from Fluka. Medium molecular weight chitosan and acetic acid were purchased from Sigma-Aldrich and Riedel-de haen, respectively. PBS was purchased from Hyclone. Blank antibiotic discs and ampicillin were purchased from Oxoid Ltd. and AppliChem, respectively. All chemicals were used as received without further purification.

4. METHOD

4.1. PREPARATION OF BACTERIA SAMPLES

E. coli and *Staphylococcus cohnii* were obtained from our microorganism collection (Yeditepe University, Genetics and Bioengineering Department). Both bacteria were verified by the Microbial Identification System (MIDI). They were subcultured three times for 24 h at 37 °C on 16 mL NA (Peptone from meat 5,0 g/L; Meat extract 3,0 g/L; Agar-agar 12,0 g/L) and TSA (Peptone from casein 15,0 g/L; Peptone from soymeal 5,0 g/L; NaCl 5,0 g/L; Agar-agar 15,0 g/L) before their use. *E.coli* and *S.cohnii* were inoculated with streak plate method onto the NA and TSA media, respectively. Both bacteria were incubated for 3-48 h after inoculation.

4.2. PREPARATION OF COLLOIDAL SILVER NANOPARTICLES

AgNPs were prepared by method known as Lee and Meisel, based on the reduction of AgNO₃ with sodium citrate [92] Briefly, a 90 mg of AgNO₃ was dissolved in 500 mL distilled water and this solution was heated until boiling. A 10 mL aliquot of 1 per cent sodium citrate was added drop wise into the boiling solution and boiling maintained until the volume was reduced to the half of the initial volume. The prepared AgNP colloidal suspension is referred to as 1x. The AgNP suspension was characterized with UV/Vis spectroscopy, Dynamic Light Scattering (DLS, Zetasizer), SEM, and TEM. The maximum absorption of AgNP colloidal suspension was determined as 450 nm with UV/Vis Spectroscopy, which is characteristic for AgNP colloidal suspension with an average of 60-nm-diameter. The AgNP colloidal suspension was concentrated by centrifugation at 5500 rpm for 30 min and the concentration was brought to 4x by removing a portion of supernatant.

4.3. PREPARATION OF CHITOSAN COATED AgNPs AND BACTERIAL SAMPLES FOR SERS MEASUREMENT

A 30 mg of chitosan was dissolved in 10 ml of 1 per cent acetic acid solution and from this solution, 100 μ l was mixed with 1 ml of AgNP colloidal suspension (4x). The mixture was incubated for 1 h while shaking at room temperature. Prepared nanoparticles were characterized with UV/Vis spectroscopy, Dynamic Light Scattering (DLS, Zetasizer), scanning electron microscopy (SEM) and TEM. A 10 μ l of c-AgNPs was dropped onto biofilm-bacteria complex on the culture plates and waited for a few minutes for the c-AgNPs to come into contact with the biofilm components. This procedure was repeated for different incubation times and the culture plate was kept at room temperature until the SERS measurement, which was performed immediately after placement of suspension of c-AgNPs. Whole procedure from the placement of colloidal suspension onto the culture plate to the end of SERS measurement was about 25 minutes. Figure 4.1 shows the illustration of experiment for SERS.

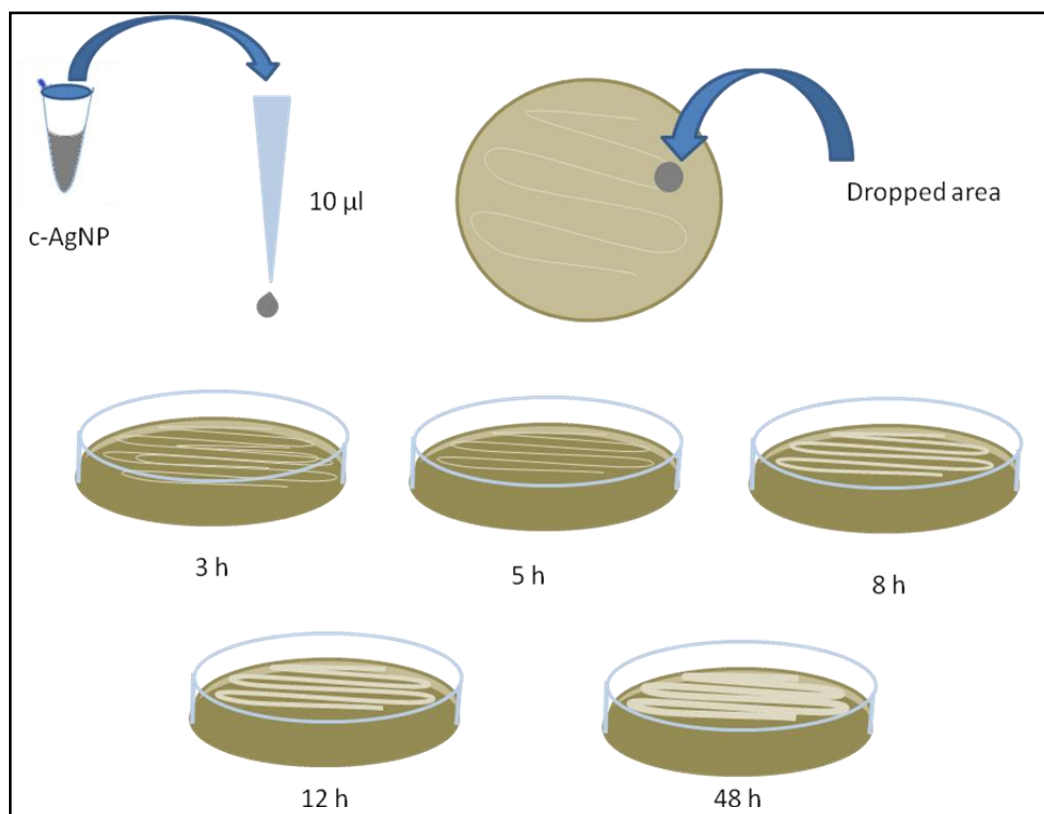


Figure 4.1. Preparation of bacterial samples for SERS acquisitions

4.4. MONITORING DEATH OF *E. COLI* EXPOSED TO AN ANTIBIOTIC

Four different ampicillin concentrations, which were 50.0, 10.0, 2.0, and 0.2 mg/mL, were used in the study. The bacteria were cultured for 8 h until they reach the logarithmic phase. Then, a 5 μ l of ampicillin solution was spotted onto the bacteria on the culture plate. The c-AgNPs were dropped and SERS spectra were acquired every 2 h after 5th h and 6th h for 2.0-mg/mL and 0.2-mg/mL-ampicillin, respectively. Average of 10 spectra was taken for each incubation time (Figure 4.2).

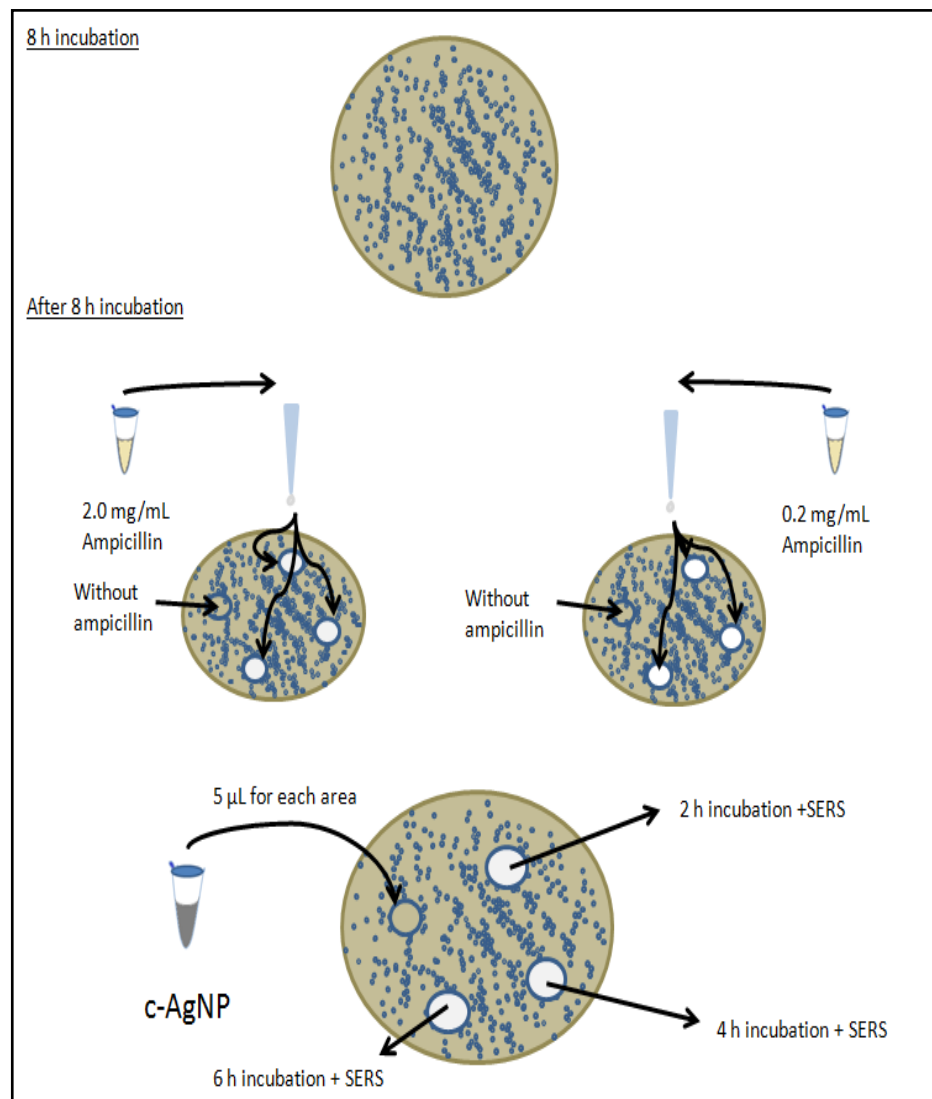


Figure 4.2. Preparation of bacterial samples in the presence of ampicillin for SERS acquisition

4.5. CONSTRUCTION OF GROWTH CURVE OF *E.COLI*

A small-scale bacteria culture was first prepared. A single colony of *E.coli* was suspended in 0.5 mL PBS and it was adjusted to 0.5 McFarland standard. The bacteria suspension was used for inoculation in a 5 mL of nutrient broth (NB). The tube was incubated at 30 °C overnight and it was used as a seed culture. Two 250 mL conical flask containing 25 mL sterile NB (10:1) were prepared to observe growth profile of *E.coli* in the presence of 2.0 and 0.2 mg/mL ampicillin for large-scale broth culture with maximum aeration. The seed culture was diluted 1:20 in conical flasks and incubated at 30 °C. A 1.5 mL of the diluted sample was taken for 11 h with 1 h intervals and OD was measured at 550 nm. The sterile medium, NB, was used as blank.

4.6. ANTIBIOTIC SUSCEPTIBILITY OF *E.COLI*

4.6.1. Disc Diffusion

Single colony of *E.coli* was suspended in 2 mL of PBS. This suspension was compared with 0.5 McFarland standard. The bacterial cells were taken with a swab and streak on the culture plate. The antibiotic discs with the four different ampicillin concentrations; 50.0, 10.0, 2.0, and 0.2 mg/mL, were placed on the culture plate and incubated overnight at 30 °C. Zone radius of each disc was measured to assess the effect of the antibiotic.

4.6.2. Effect of Antibiotic in the Growth of *E.coli*

A small-scale bacteria culture was prepared as mentioned above. After 8 h, 2.0 mg/mL and 0.2 mg/mL ampicillin were respectively added into flasks that contain the same growth media. The optical density (OD) was continued to measure at 550 nm.

4.7. RAMAN MICROSCOPY SYSTEM

The SERS experiments were carried out with an InVia Reflex model Raman Microscopy system (Renishaw. UK). The system was automatically calibrated against a silicon wafer band at 520 cm⁻¹. A diode laser at 830 nm and 50x objective with a laser power of 3 mW

was used for all SERS experiments. The exposure time of laser on the sample was 10 s. The SERS experiment was repeated at least 3 times for all selected incubation periods and at least 5 spectra from each sampling were acquired. For the reproducibility experiment, the 10 spectra were acquired from the same sample from varying locations.

4.8. SEM MEASUREMENT

All SEM images were obtained with a Carl Zeiss Evo 40 instrument at a potential of 10 kV.

4.9. TEM MEASUREMENT

TEM images were obtained by using JEOL-2100 HR-TEM operating at 200 kV (LaB6 filament).

4.10. ZETA SIZE (DLS and ZETA POTENTIAL ANALYSIS)

The size and zeta potential analysis were performed using Zetasizer NanoZS (Malvern, UK). It is equipped with a 633 nm 4 mW He-Ne laser.

5. RESULTS AND DISCUSSION

5.1. IN-SITU MONITORING OF BIOFILM FORMATION BY USING SERS

The synthesized and coated AgNPs were characterized with SEM, TEM, UV/Vis Spectroscopy and dynamic light scattering (DLS). Figure 5.1 shows the a. SEM images, b. TEM images, c. UV/Vis spectra and d. DLS spectra before and after coating the AgNPs. As seen, the AgNPs form aggregates on the glass surface from its droplet of suspension after the evaporation of water while chitosan coated AgNPs are quite well distributed, which indicates dramatic change in their surface properties. The TEM images also show that a thin layer of chitosan is formed after the coating procedure. The UV/Vis spectra and DLS spectra show that the hydrodynamic diameter of the AgNPs increases to 80 nm from 60 nm upon coating with chitosan. This indicates that about an average of 10 nm coating is achieved onto the AgNP surface. The adhesion of chitosan could be both through physical adsorption and chemical bonding of free $-NH_2$ groups in the structure of chitosan to the AgNP surface [92]. The citrate reduced AgNPs have a negative surface potential due to the presence of negatively charged citrate ions on the surface and chitosan has a positive net charge, therefore a degree of electrostatic interaction between chitosan and AgNPs is expected. While the zeta potential of AgNPs is -46.0 before coating, it becomes 46.7 after coating, which indicates the completion of the coating process of the AgNPs.

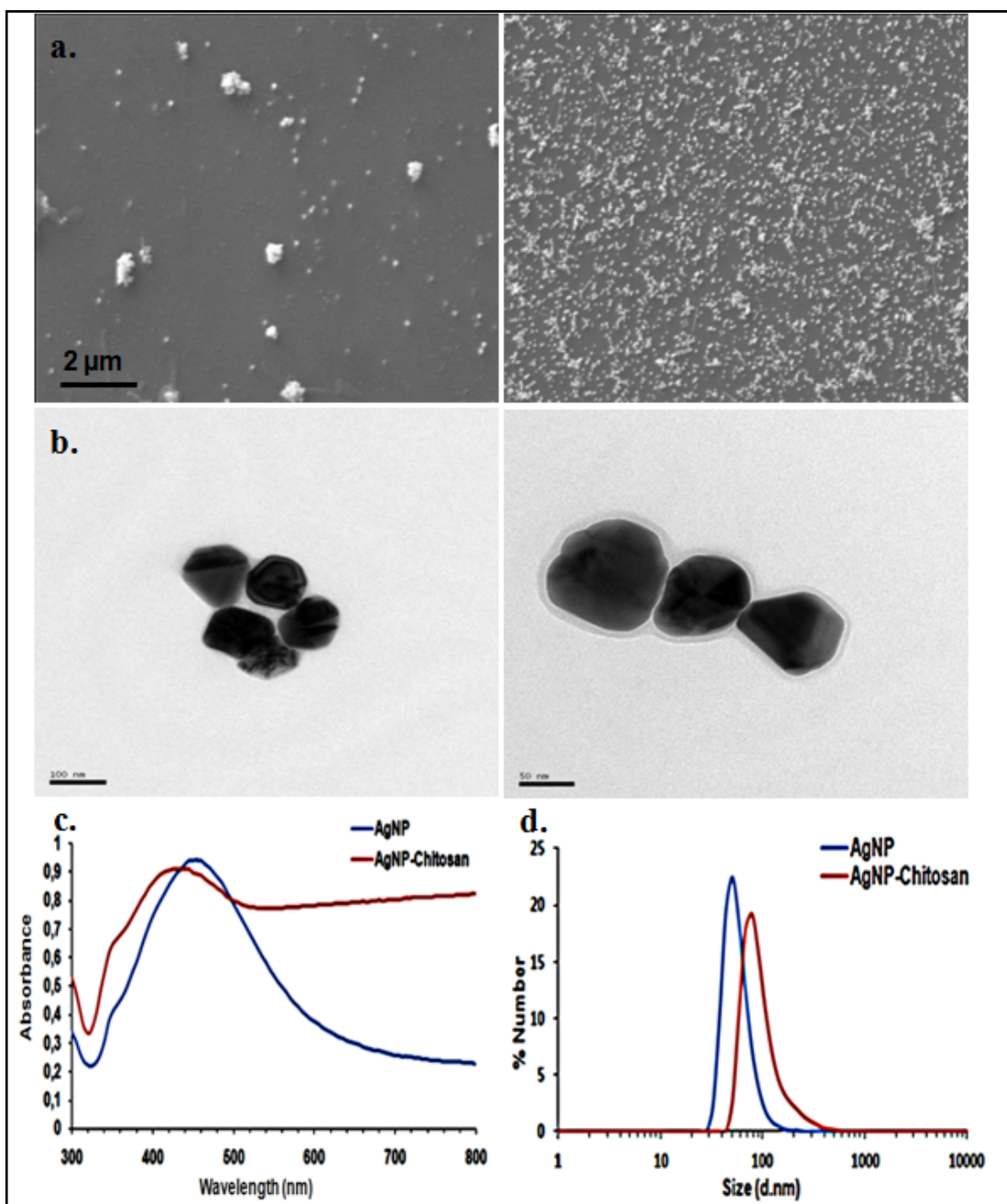


Figure 5.1. a. SEM image, b. TEM image, c. UV/Vis spectra and d. dynamic light scattering (DLS) spectra of AgNPs before and after coating. SEM and TEM images were taken from AgNP and c-AgNP droplets on the glass surface after it was dried at room temperature

Next, the possible interferences from the chitosan coat and the growth media to the SERS spectra were investigated. Figure 5.2 shows the SERS spectra of chitosan coated AgNPs themselves, and after their addition onto the growth media; nutrient agar (NA) and tryptic

soy agar (TSA) without the presence of bacteria. As seen, the bands on the SERS spectrum of chitosan coated AgNPs are very weak and different from the spectra obtained from the one obtained on the growth media. The two very weak bands on the chitosan coated AgNPs were observed at around 925 and 1050 cm^{-1} , which are attributed to C-C skeletal of chitosan and citrate, respectively. It is interesting not to observe any bands originating from C-N or N-H vibrations. When the SERS spectra obtained from both growth media are compared, some spectral similarities are observed. The bands at around 730, 1000, 1019 and 1321 cm^{-1} , which are common for both growth media, can be assigned to glycosidic ring of polysaccharide, phenylalanine, C-C stretch, amide III, respectively, resulting from the components of the growth media.

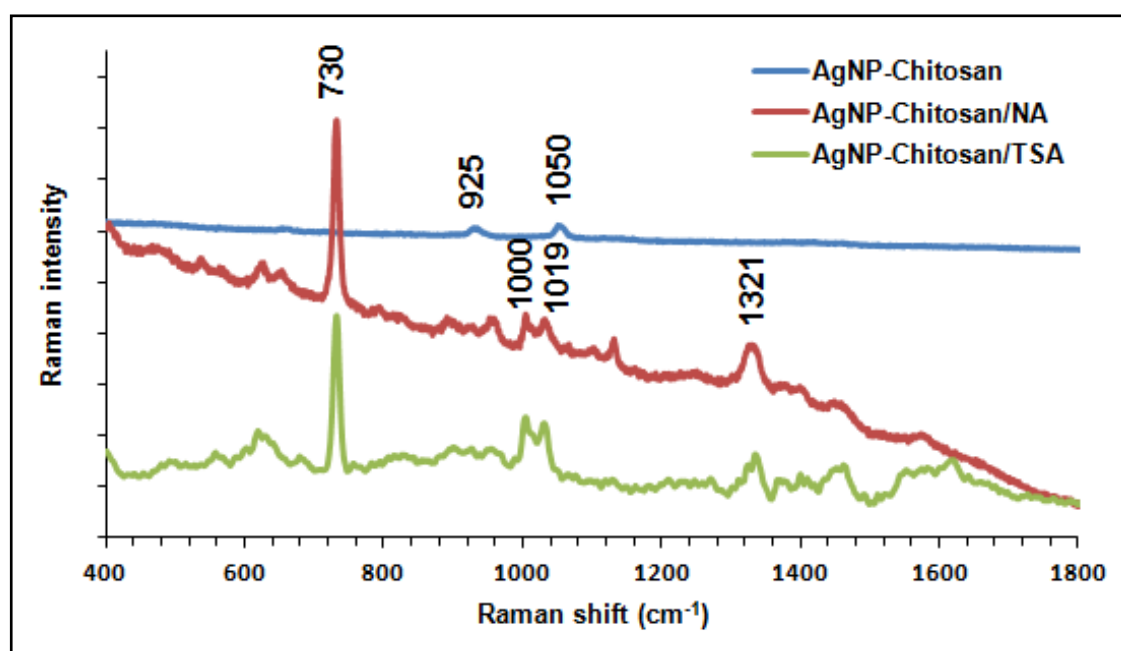


Figure 5.2. SERS spectra of c-AgNPs, after their addition onto nutrient agar (NA) and tryptic soy agar (TSA). Each spectrum is the average of five spectra acquired from the sample

The biofilm formation using two model bacteria, *E. coli* and *S. cohnii*, was investigated by monitoring the changes on the SERS spectra during the growth of bacteria. A 10- μL volume of colloidal suspension of c-AgNPs was placed onto the bacteria on the culture plate. First, the reproducibility of the SERS spectra obtained directly from the culture plate was evaluated. The c-AgNPs and their aggregates were randomly distributed on the spotted

area and it was important to realize where the laser spot was placed on the aggregates on the culture plate. Figure 5.3 shows the reproducibility of the spectra obtained from the biofilms of a. *E. coli* and b. *S. cohnii*. Inset shows the image of a chitosan-AgNP spotted region under 50x objective.

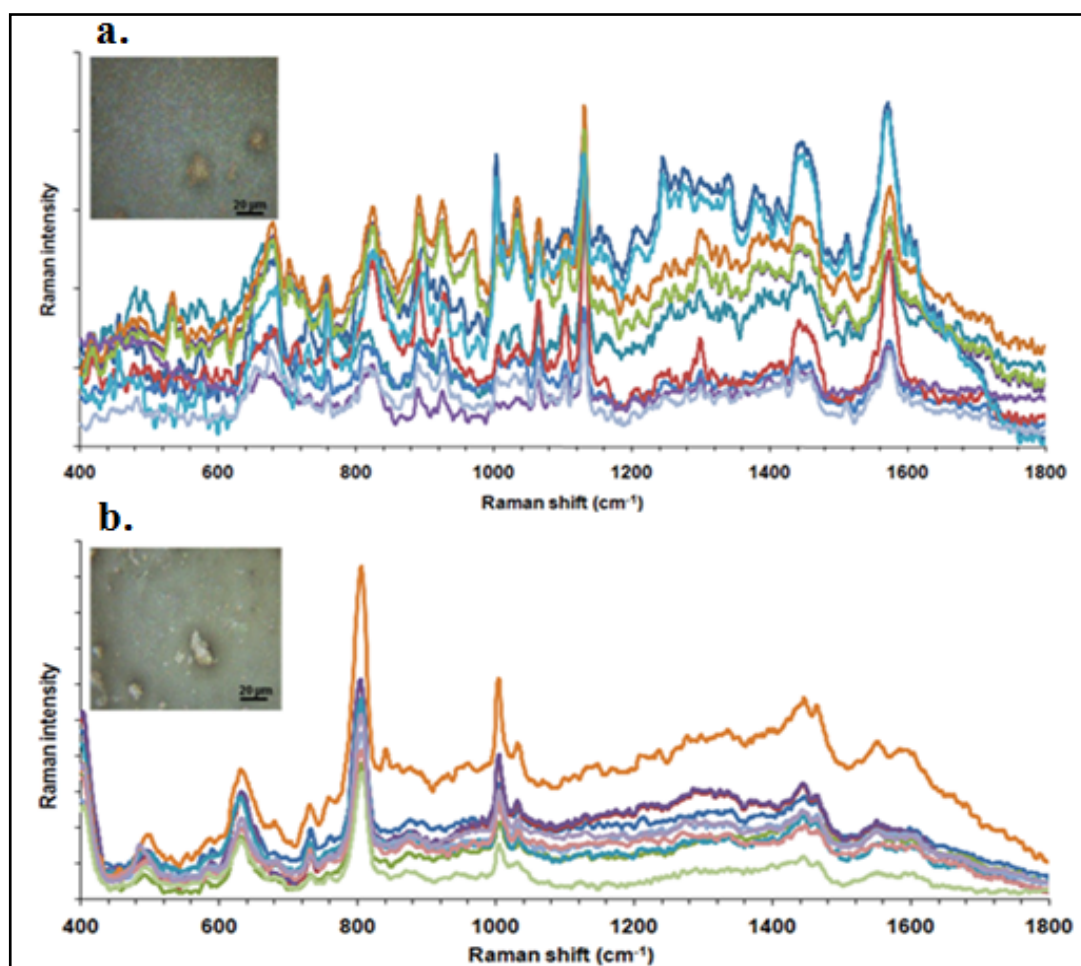


Figure 5.3. Reproducibility of SERS spectra of a. *E. coli* and b. *S. cohnii*. Inset images are white-light image of c-AgNP aggregates on culture plate. Ten spectra are collected from arbitrarily chosen locations on the colloidal droplet area

Since the AgNP aggregates scatter light in the visible region of the spectrum very effectively, it is rather easy to locate the aggregates under the light microscope objective [23]. The regions where the AgNP aggregates concentrated were chosen for the acquisition of the SERS spectra. The most important point at this stage was the spectral reproducibility obtained from such chaotically distributed AgNP aggregates. Figure 5.3 shows the

reproducibility of the SERS spectra for both model bacteria. Although there are fluctuations in the base line, the spectral variations are reasonably good for the purpose of the study. The fluctuations in both base line and spectra are the results of varying number of AgNPs and their aggregates under the laser spot as the laser is moved around on the sample.

Finally, we monitored that the changes in the biofilm composition with increasing incubation time using c-AgNPs as SERS probes. Figure 5.4 shows the changes on the SERS spectra of the biofilm of *E. coli* with during its growth (from 3 to 48 hours). As seen, several spectral changes are observed on the spectra as the bacteria continue to grow. Although most of the peaks on the spectra can be attributed to more than one biomacromolecule, the changes in the intensity or the shape of the bands can be related to the changes in the concentration of the biomacromolecules. The bands a change observed are marked on the spectrum with an asterisk. The band assignments are provided in Table 5.1.

Table 5.1. Tentative band assignments on the SERS spectra acquired from biofilm using c-AgNPs

<u>Raman Band</u> (cm^{-1})	<u>Assignment</u>
484	Carbohydrate ⁹³
650	Tyrosine ⁹³
678	ring breath modes in the DNA bases ⁹⁷
730	peptidoglycan structure and/or DNA ^{23,88,94}
758	symmetric breathing of tryptophan ¹⁰⁰
802	uracil-based ring breathing mode ¹⁰⁷
820	Protein ⁹⁸
870	single bond stretching vibrations for amino acids proline, valine ¹⁰²
884	Protein, including collagen I ¹¹²
925	C-C stretch of proline ring/glucose or lactic acid ^{100,110}
1000	Phenylalanine ¹¹¹
1024	Carbohydrates, Glycogen ¹⁰⁸
1111	Benzoid ring deformation ⁷⁶
1129	$\nu(\text{C-C})$ skeletal of acyl backbone in lipid ¹⁰³
1240	RNA ^{97,110}
1300	CH_2 bend ^{100,101,109}
1430-1440	CH_2 defect ^{100,101}
1460	CH_2CH_3 deformation of lipids and collagen ¹⁰³
1570	DNA, DNA components or RNA ⁹³

A variation in the concentration of biomacromolecules such as carbohydrates, lipids, proteins and DNA/RNA components is expected as a result of fundamental molecular activities of microorganisms. Since chitosan carries $-\text{NH}_2$ groups in its structure, it is plausible to expect that the c-AgNPs interact with mostly negatively charged species

present in the growth media. However, the bands at 484 and 1024 cm^{-1} are attributed to carbohydrates [93]. An observable decrease and a slight decrease in the intensity of the bands at 484 cm^{-1} and 1024 cm^{-1} , respectively, at 8 and 12 h incubation periods are observed. This can be related to the change in the concentration of carbohydrates during the increased anabolic activity at the log-phase.

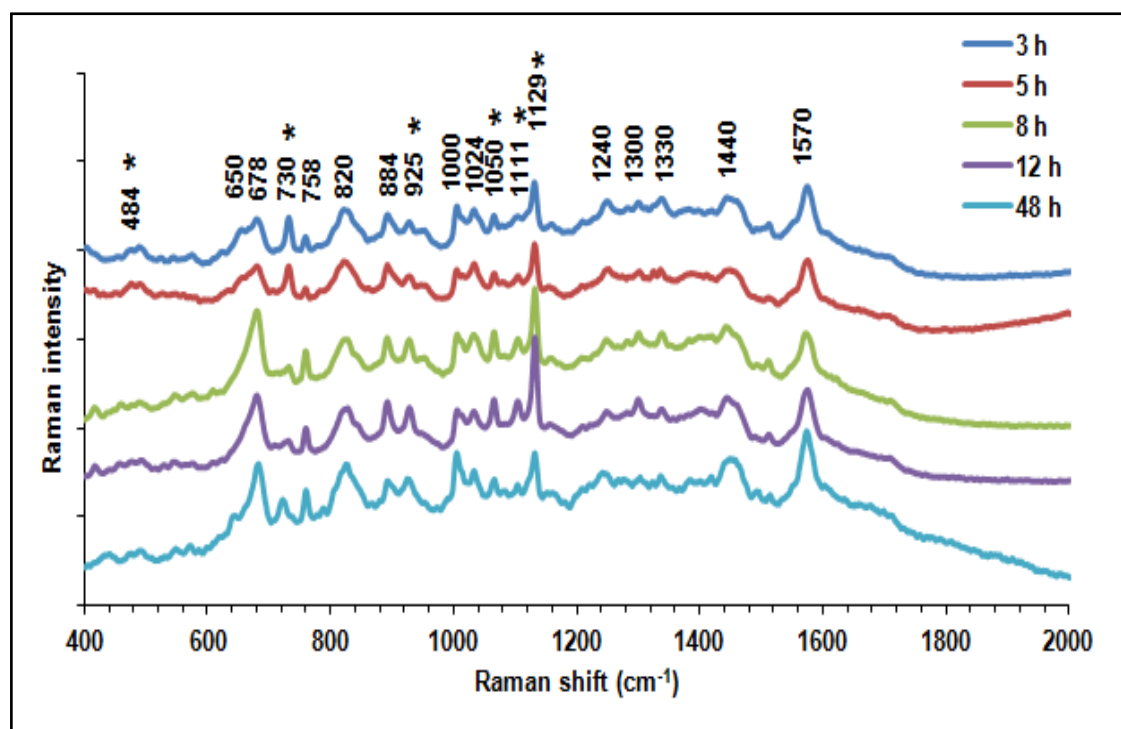


Figure 5.4. SERS spectra of *E. coli* biofilm during incubation time from 3 to 48 h. Each spectrum is the average of five spectra obtained from the same droplet area on the culture plate

As mentioned above, since DNA/RNA components carry significantly high density of negative charges in their structure due to the polyphosphate groups, it is expected to observe some bands originating from such structures. Therefore, we acquired SERS spectra from 20-base long oligonucleotides of A, T, G and C on c-AgNPs (Figure 5.5). Note that the mode of interactions of each species in the biofilm structure will be rather different with the c-AgNPs in such complex media compared to the interaction of each component separately. However, the SERS spectra obtained from separate molecular structures may help to better understand the origin of the band. The bands at 678, 730, 792,

925, 1104, 1332, 1573 cm^{-1} on the SERS spectra of oligonucleotides can be related to the bands on the SERS spectra of the biofilm. The change in the intensity of the band at 678 cm^{-1} along with the band at around 1570 cm^{-1} can be related to the concentration changes of DNA/RNA or their components in the biofilm since these bands are observed on the guanine spectrum (Figure 5.5).

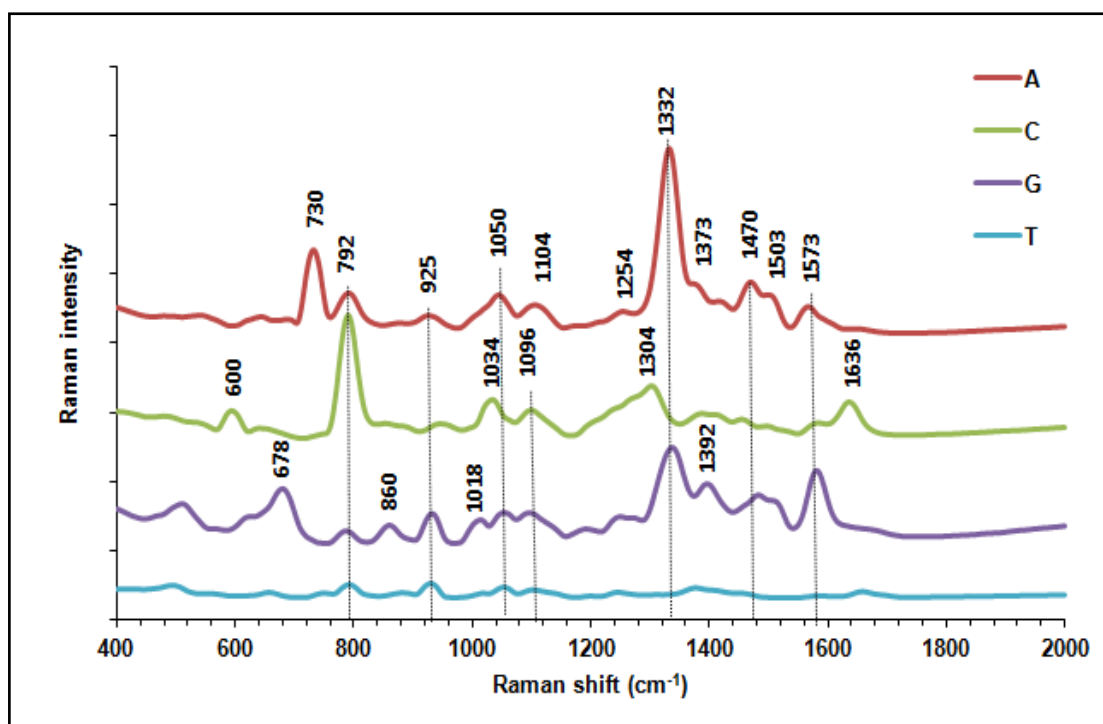


Figure 5.5. SERS spectra of nucleic acid bases, A, C, G and T. Each spectrum is the average of five spectra acquired from each sample

The spectra obtained at 3 and 5 h incubation times are rather similar to each other. However, when the time is increased to 8 h, the two bands at around 650 cm^{-1} and 678 cm^{-1} merges, and the intensity of this band dramatically increases. The shape and intensity do not change significantly as the incubation time increases. When the growth phases of microorganisms were considered, the metabolite production is different in the different growth phases. During the lag-phase, bacteria start to biosynthesize RNA, ribosome and proteins based on availability of water and other ingredients from their environments. Towards the end of the lag phase, the amount of DNA increases in the biofilm. On the other hand, when bacteria pass through the exponential phase (log-phase), the DNA synthesis exponentially increases as a significantly high metabolic activity and growth rate

[34]. The merging of these two bands at 8 h incubation time may be due to transition of bacteria from lag-phase to log-phase, which is the result of the increased DNA concentration in the biofilm. The decrease in the band intensity ratio of $678/650\text{ cm}^{-1}$ at 48 h incubation time may indicate the transition from log-phase to stationary phase.

The origin of the band at 730 cm^{-1} is not clear and it is attributed to both peptidoglycan structure of bacterial cell wall and/or DNA [23, 88, 94]. Although this band is intensely observed on the *E. coli* SERS spectrum upon using citrate reduced AgNPs [23], it is not very intense on the spectra obtained in this study. This is possibly due to the presence of a chitosan layer on the AgNPs, which prevents the direct contact of AgNPs with the bacteria surface. The intensity of the band at 730 cm^{-1} varies from 3 h to 48 h. Its intensity gradually decreases from 3 h to 12 h but an increase in its intensity at 48 h is observed. The changes in this band intensity can be attributed to a few different reasons. First, as seen on Figure 5.2, this band can originate from the culture media as interference. Since the density of the bacterial cells on the culture plate is not enough to cover the media culture, the c-AgNPs come to contact with the culture media. As the incubation time increases to 12 h, there is enough number of cells on the surface preventing the contact of the c-AgNPs with culture media. At 48 h incubation time, this band reappears; the reason for this could be the death of bacterial cells allowing the AgNPs come into contact with the culture media or the degraded bacterial components including genetic material. The metabolic products as a result of the growth were generally observed at during the log phase [95, 96]. Metabolites that produced during the log phase may be toxic for bacteria and this may result in damage to the bacterial cell wall.

The bands at 758, 820, 884, 1000 and 1600 cm^{-1} can also originate from the proteins or protein containing structures such as peptidoglycans [97-99]. The intensity of the band at 758 cm^{-1} slightly increases at increased incubation times and this increase can correlated with the increased hydrophobicity of the tryptophan environment as water molecules evaporate from the growth media [100]. The intensity of the bands at 925, 1050, and 1111 cm^{-1} also increases after 5 h incubation. The bands at 925, 1050, 1111 cm^{-1} with increasing intensities up to 48 h indicate the increase in the amount of lactic acid as a result of metabolic activities of bacteria. The citrate ions on the surface of AgNPs or benzoid ring deformation can also be the source of bands, 1050, 1111 cm^{-1} , respectively. With the 48 h

incubation, the number of bands are reduced and the pattern were rather different from those observed with shorter incubation times. This might be due to the saturation of surface the NPs by the biofilm components. Besides, since the biofilm formation is almost complete at 48 h, the AgNPs added onto the biofilm may not penetrate into the biofilm as it is in the shorter times.

The bands at around 1129, 1300 and 1460 cm^{-1} may indicate the presence of lipid ($-\text{CH}_2-$ vibrations) in biofilm composition [101-103]. The phospholipid composition of biofilm altered during transition from exponential growth phase of *E. coli* to the stationary phase [104]. A dramatic increase in the intensity of the band at 1129 cm^{-1} for 8 and 12 h incubation may be the result of the increased bacterial cell population.

Figure 5.6 shows the SERS spectra obtained during the biofilm formation of *S. cohnii* with increasing incubation times from 3 h to 48 h. The rapid decrease in the intensity of 484 cm^{-1} band at 48 h incubation period after its increased intensity at shorter incubation times may be a sign that indicates the beginning of the secondary metabolite production, which is an indication of transition to the stationary phase as discussed above. The band at 678 cm^{-1} (ring breath modes in guanine) can give information about the total DNA/RNA concentration in biofilm structure [105,106]. This band was observed for all incubation periods. From its intensity, it is possible to conclude that the highest DNA/RNA concentration is observed for 8 and 12 h incubation periods. The band at 802 cm^{-1} attributed to the ring-breathing mode of uracil, which is a components of RNA [107] and its intensity suddenly increases when the incubation time reaches to 48 h. The intensity increases can be considered as the increase in the concentration of RNA. The other reason could be the change in the vibrational mode of uracil ring as a result of interaction of water molecules with RNA, which has an important effect on the vibration of uracil ring [107]. When the band at 678 cm^{-1} is compared to the band at 802 cm^{-1} , there is an increasing trend in their intensity until 48 h incubation suggesting that the bacteria is still in the same growth phase. During the exponential growth phase, DNA is synthesized more than RNA as a result of the bacterial multiplication [34].

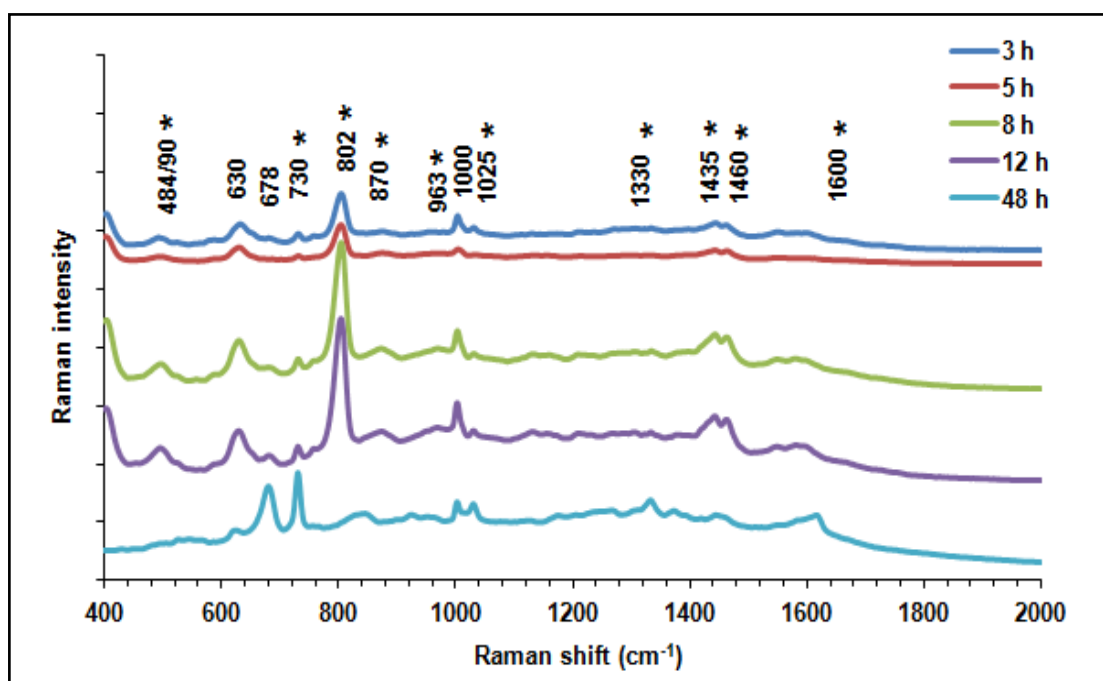


Figure.5.6...SERS spectra of *S. cohnii* biofilm during incubation time from 3 to 48 h. Each spectrum is the average of five spectra obtained from the same droplet area on the culture plate

After 8 h incubation, a very intense band at around 870 cm^{-1} emerges and disappears after 48 h incubation. The band is most probably due to single bond stretching vibrations of amino acids proline and valine [97]. The loss of the band at 48 h incubation may also correlate with the rapid log-phase result in the transition to the stationary phase. The band at 963 cm^{-1} may be due to out-of-plane bending. The bending vibrations give information about changes in the position of the atoms, which affects their original bond axes. The bands at 1435 cm^{-1} and 1460 cm^{-1} (CH_2CH_3 deformation of collagen) [101] were observed until 12 h incubation and disappear after 48 h incubation. Although there is a large change in the composition of biofilm, the band at 1435 cm^{-1} becomes more apparent at 3 h incubation. Finally, the band at 1600 cm^{-1} (Amide I band of proteins) [93, 108] become visible at 8 h incubation. The band at 1129 cm^{-1} ($\nu(\text{C-C})$ skeletal of acyl backbone in lipid) which was observed on the spectra of *E. coli* was not observed in *S. cohnii*. These may be due to the structural differences between two bacteria types.

When the SERS spectra of both types of bacteria (Gram – and Gram +) are compared, it is clear that they generate biofilms with significantly different compositions. While the SERS spectra obtained from the biofilm of *E. coli* (Gram -) are rich in spectral features indicating the diversity of the biomacromolecules in the biofilm, the spectra obtained from the biofilm of *S. cohnii* have fewer spectral features suggesting the less complex metabolic activity.

5.2. OBSERVATION OF BACTERIAL DEATH FROM SERS SPECTRA

It is important to be able obtain *in situ* information during the growth of microorganisms since some of the important molecular information during the transfer of the microorganism from culture media (for example, washing) can be lost. In previous studies, microorganisms were brought together with SERS substrate upon their culture for certain time. In this part of the study, the spectral changes on the SERS spectra during the death of bacteria in the presence of ampicillin antibiotic were investigated to relate to the biochemical changes during the death. Therefore, the effect of different antibiotic concentrations on the morphology of bacterial cell wall was monitored.

First, the growth profile of *E. coli* and the effect of antibiotic on *E. coli* growth were established by measuring the optical density of broth culture media at 550 nm (OD_{550}). The initial turbidity was adjusted to McFarland standard and measurements were taken in 2 h intervals during 12 h until the OD_{550} reaches a plateau. The first measurement was taken after 2 h incubation to achieve sufficient turbidity on media. The measured growth profile of *E. coli* is presented in Figure 5.7. as seen, the curve is very typical for bacteria and is composed of three different regions, the lag, the log and stationary phases, respectively.

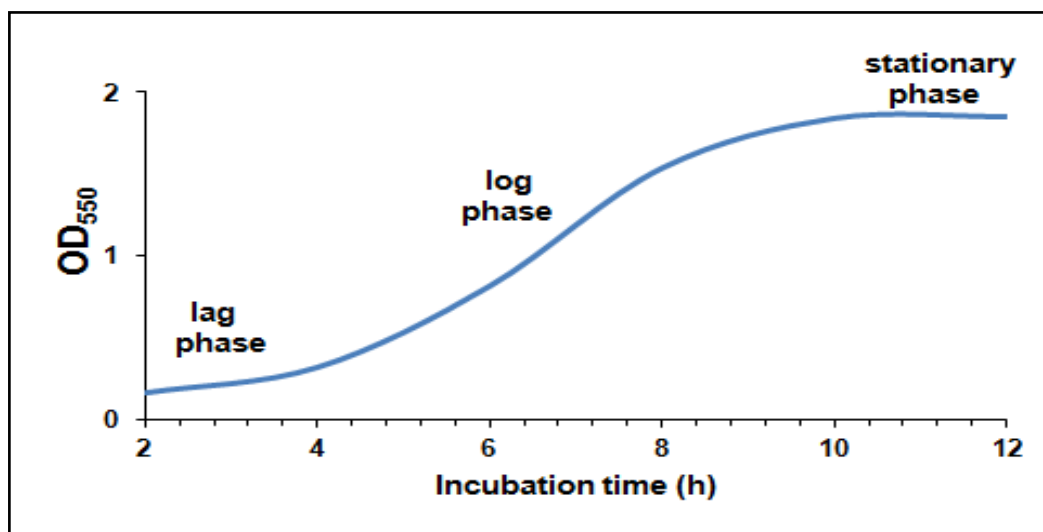


Figure.5.7.The growth profile for *E.coli* at OD₅₅₀

In this study, we have chosen to use the penicillin group beta-lactam antibiotic, ampicillin. The act of ampicillin on Gram-positive and some Gram-negative bacteria is through the penetration into the cell wall [113]. *E. coli* were exposed to four different antibiotic concentrations in order to determine the study concentration. For this, the disc diffusion technique, in which the diameter of the zone of formed around the disc slowly releasing antibiotic into the culture media was used for the assessment, was employed. The inhibition zone diameters were measured as 20 mm for 50.0 mg/mL, 10 mm for 10.0 mg/mL, 6 mm for 2.0 mg/mL and finally 1 mm for 0.2 mg/mL Ampicillin (Figure 5.7). These results indicated that the 50.0 mg/mL ampicillin solution completely prevented the growth of *E. coli*. The effect of concentration at 10.0 mg/mL ampicillin was also significant on *E.coli*. The concentrations lower than 10.0 mg/mL did not have a substantial effect on the bacterial growth.

Since the effect of concentrations at 50 and 10 mg/mL was dramatic, we chose the lower concentrations, 2.0 mg/mL and 0.2 mg/mL, for further study. Next, the effect of ampicillin on *E. coli* at these lower concentrations was investigated. The equal amounts of *E.coli* were inoculated in the culture broth, and growth profiles were recorded for 11 h. However, the antibiotic solution was added into the broth after 8 h incubation in order to provide a sufficient growth to *E.coli* and observe the death in details. As seen in the Figure 5.8, *E.coli* showed almost the same curve for both culture mediums until the ampicillin was

added (8h incubation). The 8th h measurement was taken in the presence of ampicillin and a slight separation in the growth curves was observed. In order to show the difference between the growth profiles, we focused on the area that contains until stationary phase.

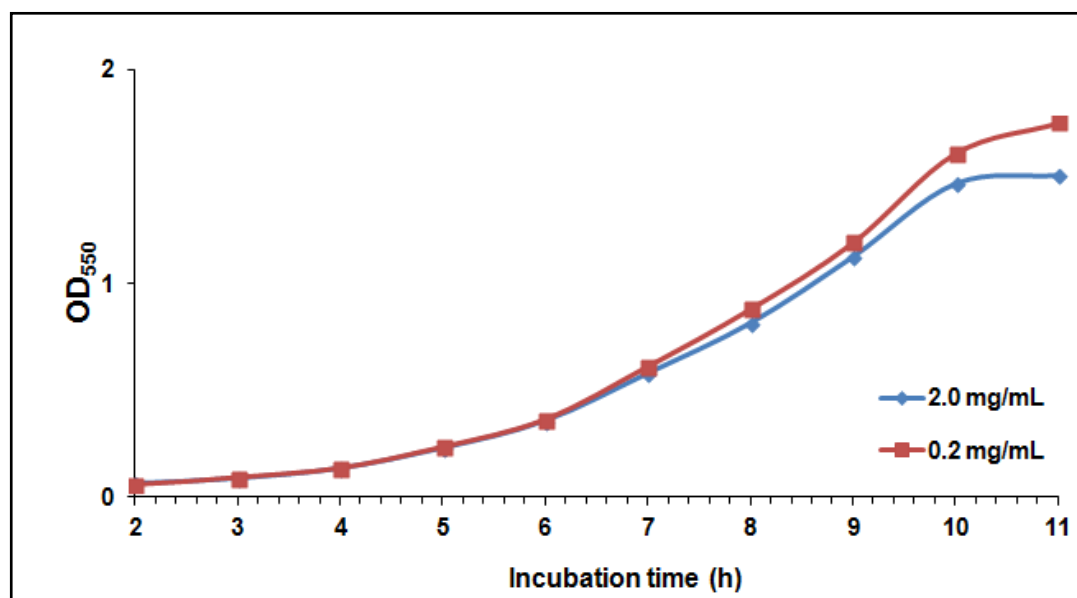


Figure 5.8. The growth profile of *E.coli* in presence of 2.0 mg/mL and 0.2 mg/mL ampicillin

Finally, the determination of growth profile and death of *E.coli* were investigated with SERS. The bacteria were cultured for 8 h until they reach to the logarithmic phase. At 8 h, a 5- μ L solution of each ampicillin concentrations of 0.2 and 2.0 mg/mL was spotted directly onto the bacteria on the culture plate. The c-AgNPs were dropped and SERS spectra were acquired for 5 h for 2.0 mg/mL and 6 h for 0.2 mg/mL ampicillin (until observing a significant change on the spectra) with every 120 minutes. Average 5 spectra were taken for each incubation time. The reproducibility of the SERS spectra obtained from the *in situ* measurement was also assessed. Figure 5.9 shows the reproducibility of the spectra for both concentrations of 0.2 and 2.0 mg/mL.

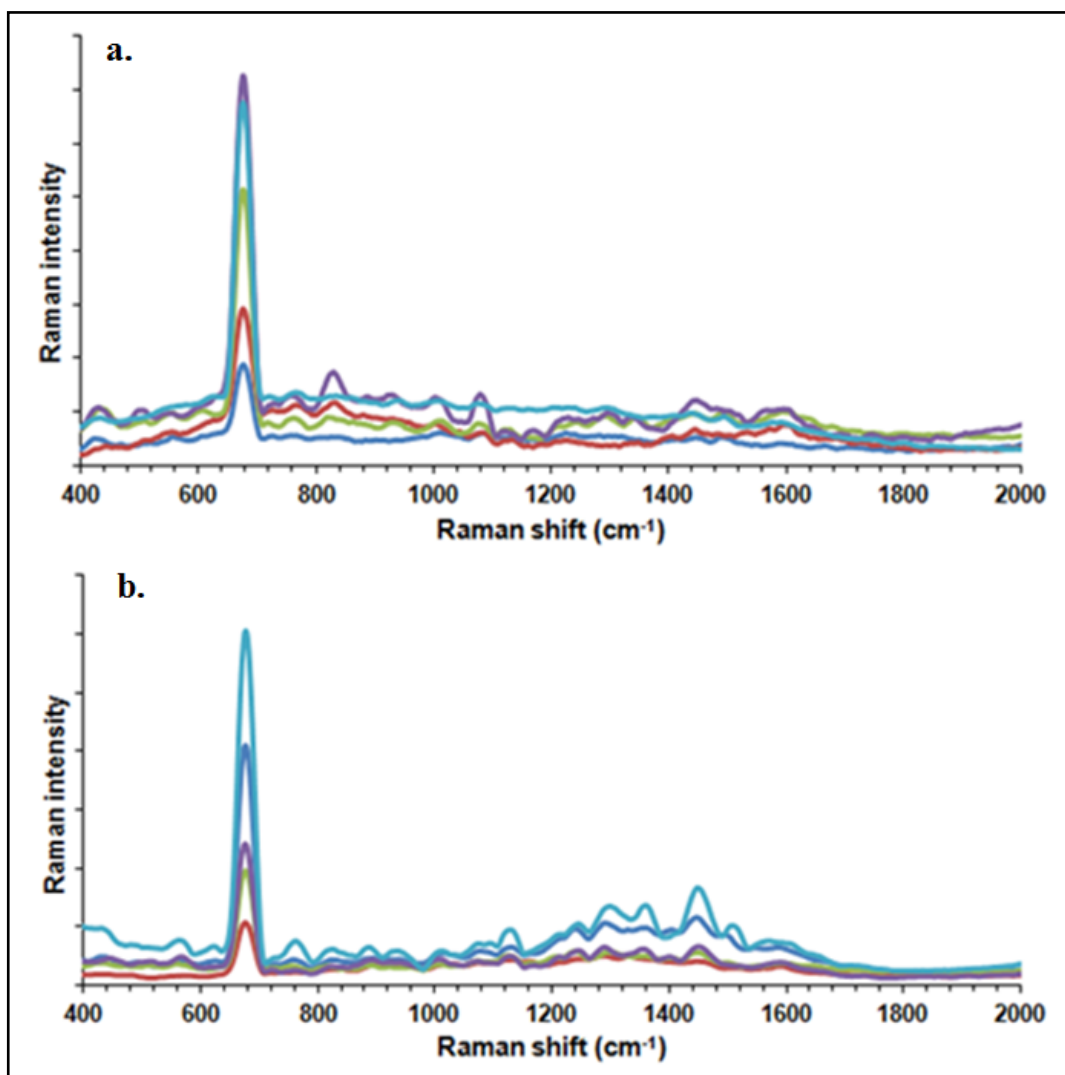


Figure 5.9. Reproducibility of SERS spectra for *E. coli* in the presence of a. 2.0 mg/mL and b. 0.2 mg/mL ampicillin at the end of incubation period for both bacteria

Although the SERS spectra show some fluctuations from point to point on the c-AgNP containing colloidal suspension spot, a quite clear and sharp peak at 678 cm^{-1} was observed on the spectra at 4 h after the addition of ampicillin solution. The intensity of the peak also showed some variation from spot to spot in the area. This could be due to the difference in the aggregation status of the AgNPs as the colloidal suspension was spotted onto the culture media.

Finally, the spectral changes observed on the SERS spectra during the bacterial death were evaluated at two concentrations of ampicillin, 0.2 and 2.0 mg/mL. A $5\ \mu\text{L}$ of ampicillin

solution was placed onto *E.coli* culture media incubated for 8 h. A 10 μL of c-AgNP suspension was placed onto the area where includes both ampicillin and bacteria. The SERS spectra obtained during the death of bacteria at two concentrations, a. 0.2 and b. 2.0 mg/mL are shown on Figure 5.10. With the 0.2-mg/mL-concentration exposure, the SERS acquisition was performed at the end of the 2nd hour since we could not observe any change on the SERS spectra. Therefore, the SERS spectra acquisitions were performed at the end of 4th and 6th hours. With the 2.0-mg/mL-concentration exposure, the SERS spectra acquisitions were performed at the end of the 1st, 3th and 5th hours. The comparison of the SERS spectra at both antibiotic concentration levels reveals that a significant change in the biochemical composition of the environment of bacteria takes place as the bacteria are exposed to antibiotic at longer times. The biochemical changes in the environment c-AgNPs are clearly reflected by the SERS spectra. Although several new peaks appear on the SERS spectra at the end of the 5th and 6th hours for both cases, the emergence of a very intense peak at 678 cm^{-1} confirm the significant changes in the biochemical composition on the surface of the culture plate. Since this peak was quickly emerged on the SERS spectra at 50 and 10 mg/mL ampicillin concentrations, these two lower concentrations were selected for further study as indicated earlier. The spectra of *E. coli* and NA were included for comparison on the figures.

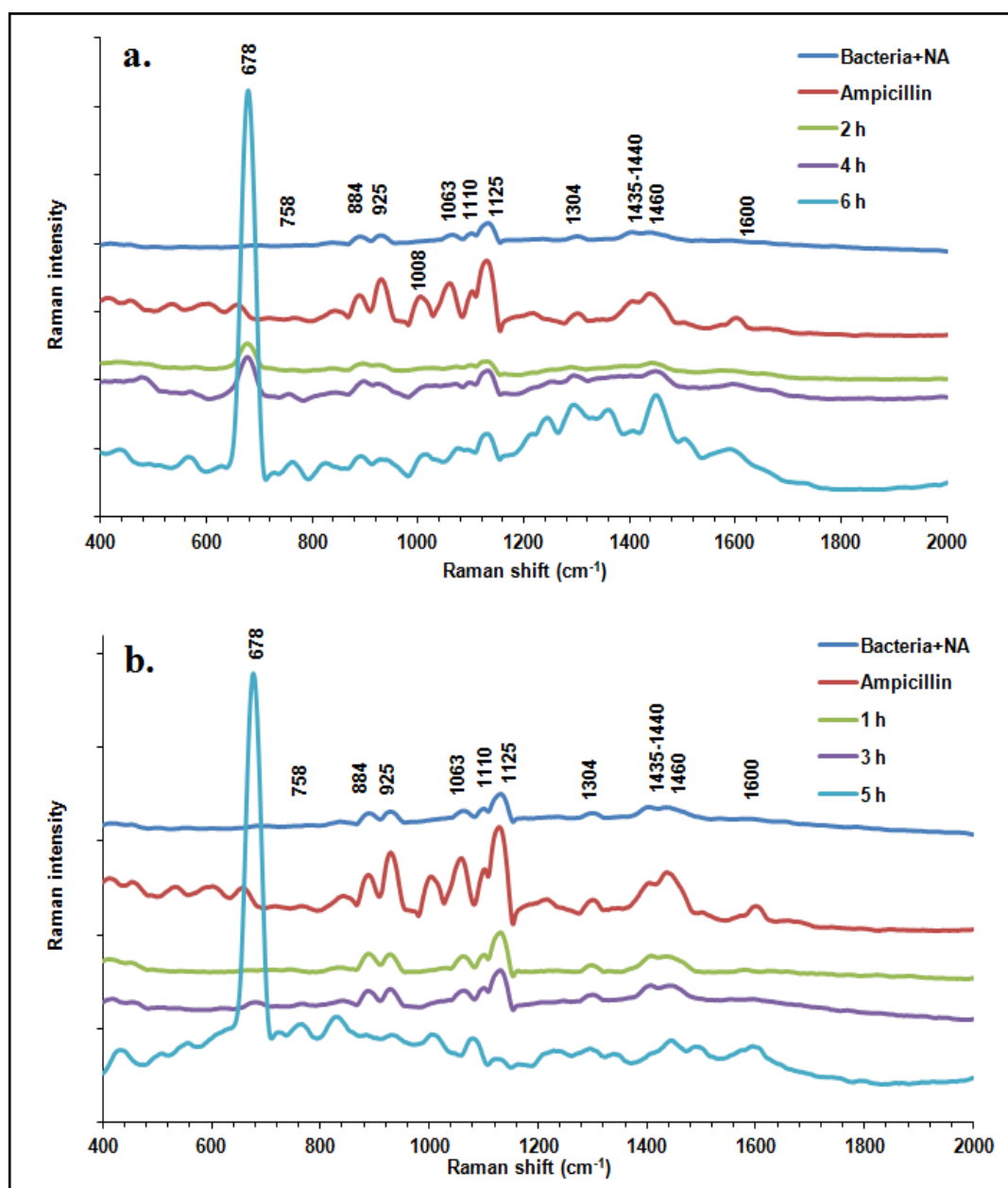


Figure 5.10. SERS spectra obtained during the death of *E. coli* with the addition of a. 0.2 mg/mL and b. 2.0 mg/mL ampicillin at different times

The intense peak at 678 cm^{-1} is attributed to the ring breathing modes in the DNA bases [93]. The other peaks at 1110 and 1125 cm^{-1} with considerably low intensity were assigned C-C and C-N vibrations, respectively. The peak at 1460 cm^{-1} indicates the CH_2 deformations [93]. The peak at around 1600 cm^{-1} is attributed the Amide I band of proteins. The band at 884 cm^{-1} originates from proteins [93]. The band at 925 cm^{-1} is attributed to C-C stretch of proline ring/glucose or lactic acid [100, 114, 115]. The peak at

1008 cm^{-1} and 1063 cm^{-1} attribute the presence of $\nu(\text{CO})$, $\nu(\text{CC})$, $\delta(\text{OCH})$, ring and C-C stretch, respectively. These bands were obtained on the spectra of ampicillin. The band at around 1110 cm^{-1} originates from benzoid ring deformation. The band at 1125 cm^{-1} is also attributed to the $\nu(\text{C-C})$ skeletal of acyl backbone originating from lipids [116, 117]. The peaks at 1008 cm^{-1} and 1063 cm^{-1} originate from of *E.coli* and ampicillin. The band at around 1304 cm^{-1} indicates the presence of CH_2 deformation, adenine and cytosine. The band at 1435 cm^{-1} attributes the CH_2 defect [93].

We attribute the changes on the SERS spectra as the incubation time increases under the antibiotic exposure to the death of bacteria. Since the action of ampicillin is through the penetration into the cell wall, it is well-possible that the observed changes on the spectra are due to the biological components disrupted from the cell wall structure and eventually leakage of the biochemical components from the inside of the bacterial cells as a result of disintegration of bacterial cells. The intensity of the peak at 678 cm^{-1} increases with bacterial death. The band at 758 cm^{-1} , which is attributed to symmetric breathing of tryptophan slightly increases during the increased incubation times. The 758 cm^{-1} band is known sensitive to hydrophobicity of its environment as mentioned before. Therefore, the observed increase for both ampicillin concentrations can be due to evaporation of water molecules from the growth media. The change in the intensity of 884 cm^{-1} can be related to the proceeding of the protein synthesis for 0.2-mg/mL-concentration. On the other hand, the band at 884 cm^{-1} disappears at 5 h incubation for 2.0-mg/mL-concentration due to the higher efficiency of concentration. An increase in the intensity of the peaks at 1304 cm^{-1} and 1435 cm^{-1} , which are attributed to proteins, were also observed with increasing incubation time.

It was reported that the peak at 678 cm^{-1} could be originating from the guanine [93,97]. In order to investigate this hypothesis, we have acquired SERS spectra from 20-base long poly A, T, G and C on the c-AgNPs. As seen in Figure 5.5, an intense peak at 678 cm^{-1} was observed on the spectra of guanine. Therefore, the observed peak on the spectra of bacteria can be originating from the guanine as bacteria are decomposed.

6. CONCLUSION AND RECOMMENDATIONS

6.1. CONCLUSION

The identification of components in a biofilm composition may clarify the mode of interaction of microorganisms with their environment during their growth. Therefore, a better understanding of the interactions of microorganisms with their environment, biofilm composition and changes in the composition during the growth has a critical importance in the several fields including medicine and biotechnology. In addition, being able to monitor the death of microorganisms in their natural environment upon their exposure to a foreign material is critically valuable for toxicity assessment efforts. For this reason, development of a method that allows *in situ* monitoring of microorganisms while they are in their natural environment can have dramatic impact in the field. In this thesis, we demonstrated *in situ* monitoring of the molecular changes during the biofilm formation using a core AgNP-shell chitosan substrate. The coated polymer on the AgNPs prevents the excessive accumulation of biofilm components that have higher affinity for the metallic silver surface, which might be problematic in such complex biological environments since the SERS spectrum is always dominated by those biological structures possessing high affinity for silver surface. The release and the change in the concentration of species such as DNA, RNA, protein, and carbohydrate during the growth phases of bacteria can easily be monitored using the presented approach. Although it is very difficult to predict the exact source of the bands on the SERS spectra of biofilms produced by two types of bacteria, the molecular information obtained from the spectra can provide valuable insight about the metabolic activities of microorganisms. From the spectral patterns of both types of bacteria, one can conclude they show very different metabolic activities. We will continue to explore the approach by extending the types of microorganisms and investigating the source of the band on the SERS spectra.

At the second part of the thesis, we demonstrated *in situ* monitoring of molecular changes during the bacterial death. The c-AgNPs were used as SERS substrate. It was found that the SERS spectra could provide significant information about the morphologic changes on the bacterial cell wall and media conditions during the death of bacteria. The release of

DNA/RNA bases as a result of decomposition of bacteria and deformations on cell wall can be easily monitored. A dramatically emerging band as the incubation time of bacteria under the antibiotic stress was observed at 678 cm^{-1} . This band clearly arises from the death of bacteria. We propose that this approach can also be used for the assessment of toxicity of molecules and nanomaterials. It is interesting to note that on the SERS spectra both type of bacteria, Gram + and –, this band emerges in a very similar fashion, which indicates the similarity of possible death mechanism.

6.2. RECOMMENDATIONS

The prepared SERS substrate (Chitosan shell & AgNP core) can be used to detect and identify various kinds of biological molecules and structures such as DNA, RNA, proteins and viruses.

In future work, the study can be applied for different bacteria types and a database for extracellular polymeric substances can be generated. The developed procedure can also be applied to bacterial mixtures. For this purpose, the microorganisms that are cultured on the same culture plate can be investigated and the changes in the biofilm composition can be identified. Therefore, ‘Quorum sensing’ and ‘Quorum quenching’ can be determined.

The death of bacteria based on their antibiotic susceptibility can be studied in a wide range of concentrations and with different antibiotics. Minimum inhibition concentration (MIC) can conventionally be determined for a range of antibiotics and the results can be compared with the results obtained with SERS study.

The methods can also be extended for toxicity assessment of molecules and nanomaterials.

7. REFERENCES

1. Donlan, R. M., “Biofilm formation: A Clinically Relevant Microbiological process”, *Healthcare epidemiology*, Vol. 33, pp. 1387-1392, 2001.
2. Vu, B., Chen, M., Crawford, R. J., Ivanova, E. P., “Bacterial Extracellular Polysaccharides Involved in Biofilm Formation”, *Molecules*, Vol. 14, pp. 2535-2554, 2009.
3. Flemming, H. C., Wingender, J., “The biofilm matrix”, *Nature Reviews Microbiology*, Vol. 8, pp. 623-633, 2010.
4. Lawrence, J. R., Neu, T. R., Swerhone, G. D. W., “Application of multiple parameter imaging for the quantification of algal, bacterial and exopolymer components of microbial biofilms”, *J. Microbiol. Methods.*, Vol. 32, pp. 253–261, 1998.
5. Zhang, T., Fang, H. H. P., “Quantification of extracellular polymeric substances in biofilms by confocal laser scanning microscopy”, *Biotechnol Lett.*, Vol. 23, pp. 405-409, 2001.
6. Lawrence, J. R., Swerhone, G. D. W., Leppard, G. G., Araki, T., Zhang, X., West, M. M., Hitchcock, A. P., “Scanning transmission X-ray, laser scanning, and transmission electron microscopy mapping of the exopolymeric matrix of microbial biofilms”, *Appl Environ Microbiol.*, Vol. 69, pp. 5543-5554, 2003.
7. Strathmann, M., Wingender, J., Flemming, H. C., “Application of fluorescently labeled lectins for the visualization and biochemical characterization of polysaccharides in biofilms of *Pseudomonas Aeruginosa*”, *J Microbiol Methods*, Vol. 50, pp. 237-248, 2002.

8. Neu, T. R., Lawrence, J. R., “Lectin-binding analysis in biofilm systems”, *Methods Enzymol.*, Vol. 310, pp. 145–152, 1999.
9. Haisch, C., Niessner, R., “Visualization of transient processes in biofilms by optical coherence tomography”, *Water Res.*, Vol. 41, pp. 2467–2472, 2007.
10. Wagner, M., Ivleva, N. P., Haisch, C., Niessner, R., Horn, H., “Combined use of confocal laser scanning microscopy (CLSM) and Raman microscopy (RM): investigations on EPS- Matrix”, *Water Res.*, Vol. 43, pp. 63-76, 2009.
11. Ivleva, N.P., Wagner, M., Horn, H., Niessner, R., Haisch, C., “*In Situ* Surface-Enhanced Raman Scattering Analysis of Biofilm”, *Anal. Chem.*, Vol. 80, pp. 8538–8544, 2008.
12. Ivleva, N. P., Wagner, M., Szkola, A., Horn, H., Niessner, R., Haisch, C., “Label-Free *in Situ* SERS Imaging of Biofilms”, *J. Phys. Chem. B.*, Vol. 114, pp. 10184–10194, 2010.
13. Smirnova, T. A., Didenko, L. V., Tiganova, I. G, Andreevskaya, S. G., Alekseeva, N. V., Stepanova, T. V., Romanova, Y. M., “Study of the structures of biofilms formed by *Salmonella typhimurium* bacteria on abiotic surfaces by the methods of light and transmission electron microscopy”, *Appl Biochem Microbiol.* , Vol. 46, pp. 706-711, 2010.
14. Hunter, R. C., Beveridge, T. J., “High-resolution visualization of *Pseudomonas aeruginosa* PAO1 Biofilms by freeze-substitution transmission electron microscopy”, *J Bacteriol.*, Vol. 187, pp. 7619-7630, 2005.
15. Ngo Thi, N.A., Naumann, D., “Investigating the heterogeneity of cell growth in microbial colonies by FTIR microspectroscopy”, *Anal Bioanal Chem.*, Vol. 387, pp. 1769-1777, 2007.

16. Venkata, H. N. N., Nomura, N., Shigeto, S., “Leucine pools in *Escherichia coli* biofilm discovered by Raman imaging”, *J. Raman Spectrosc.*, Vol. 42, pp. 1913-1915, 2011.
17. Schmid, T., Sebesta, A., Stadler, J., Opilik, L., Balabin, R. M., Zenobi, R., “Tip-enhanced Raman spectroscopy and related techniques in studies of biological materials”, *Proc. of SPIE*, pp. 7586. 2010.
18. Das, G., Mearini, F., Gentile, F., De Angelis, F., Kumar HGc, M., Candeloro, P., Liberale, C., Cuda, G., Di Fabrizio, E., “Nano-patterned SERS substrate: Application for protein analysis vs. temperature”, *Biosensors and Bioelectronics*, Vol. 24, pp. 1693–1699, 2009.
19. Carey, P. R., *Biochemical Applications of Raman and Resonance Raman Spectroscopies*, Academic Press, New York, 1982.
20. Schuster, K.C., Urlaub, E., Gapes, J. R., “Single-cell analysis of bacteria by Raman microscopy: spectral information on the chemical composition of cells and on the heterogeneity in a culture”, *J Microbiol Methods*, Vol. 42, pp. 29-38, 2000.
21. Moskovits, M., Dillella, D. P., “Surface Enhanced Raman Scattering”. In: R. K. Chang, T. E. Furtak, editors. *Spectroelectrochemistry: Theory and Practice*. New York, USA: Plenum Press, 1982. Pp .243–273.
22. Moskovits, M., “Surface-enhanced spectroscopy”, *Rev. Mod. Phys.*, Vol. 57, pp. 783-826, 1985.
23. Kahraman, M., Yazici, M., Sahin, F., Bayrak, O. F., Culha, M., “Reproducible Surface-Enhanced Raman Scattering Spectra of Bacteria on Aggregated Silver Nanoparticles”, *Applied Spectroscopy*, Vol. 61, pp. 479-485, 2007.
24. Garcia de Abajo, F. J., “Colloquium: Light scattering by particle and hole array”, *Rev. Mod. Phys.*, Vol. 79, pp. 1267-1290, 2007.

25. Abald Cela, S., Aldeanueva Potel, P., Mateo, C., Rodrí'guez Lorenzo, L., Alvarez Puebla, R.A., Liz Marzan, L.M., "Surface-Enhanced Raman Scattering biomedical applications of plasmonic colloidal particles", *J. R. Soc. Interface*, Vol. 7, pp. 435-450, 2010.
26. Pearman, W. F., Lawrence-Snyder, M., Angel, S. M., Decho, A. W., "Surface-enhanced Raman spectroscopy for *in situ* measurements of signaling molecules (autoinducers) relevant to bacteria quorum sensing", *Appl Spectrosc.*, Vol. 61, pp. 1295-1300, 2007.
27. Chao, Y., Zhang, T., "Surface-enhanced Raman scattering (SERS) revealing chemical variation during biofilm formation: From initial attachment to mature biofilm", *Anal Bioanal Chem.*, Vol. 404, pp. 1465-1475, 2012.
28. Erbacher, P., Zou, S., Bettinger, T., Steffan, A. M., Remy, J. S., "Chitosan-Based Vector/DNA Complexes for Gene Delivery: Biophysical Characteristics and Transfection Ability", *Pharmaceutical Research*, Vol. 15, pp. 1332-1339, 1998.
29. Borchard, G., "Chitosan for gene delivery", *Advanced Drug Delivery Reviews*, Vol. 52, pp. 145-150, 2001.
30. Potara, M., Baia, M., Farcau, C., Astilean, S., "Chitosan-coated anisotropic Silver nanoparticles as a SERS substrate for single-molecule detection", *Nanotechnology*, Vol. 23, e. 055501, 2012.
31. Xu, D., Gu, J., Wang, W., Yu, X., Xi, K., Jia, X., "Development of chitosan-coated gold nanoflowers as SERS-active probes", *Nanotechnology*, Vol. 21, pp. 5101, 2010.
32. Atlas, R. M., *Microorganisms in our world*, Mosby Year Book, in Wm, C. Missouri, 1995.

33. Vollmer, W., Blanot, D., de Pedro, M. A., ‘‘Peptidoglycan structure and architecture’’, *FEMS Microbiol Rev.*, Vol. 32, pp. 149–167, 2008.
34. McKane, L., Kandel, J., Bacterial Growth and Laboratory cultivation, McGraw-Hill, New York, 1996.
35. Stoodley, P., J. D. Boyle, I. Dodds, Lappin-Scott, H. M., Biofilms: community interactions and controls, BioLine, U.K, 1997.
36. Costerton, J. W., Lewandowski, Z., Caldwell, D. E., Korber, D. R., Lappin-Scott, H. M., ‘‘ Microbial Biofilms’’, *Annu. Rev. Microbiol.*, Vol. 49, pp. 711–745, 1995.
37. Douglas, A. S., Holler, F. J., Stanley, C. R, Principles of Instrumental Analysis, USA, 1992.
38. Ferraro, J. R., Nakamoto, K., Introductory Raman Spectroscopy, Academic Press, New York, 1994.
39. Sur , U. K., ‘‘ Surface-enhanced Raman Spectroscopy Recent Advancement of Raman Spectroscopy’’, *Resonance*, Vol. 15, pp. 154-164, 2010.
40. Kelf, T., ‘‘Surface Enhanced Raman Spectroscopy’’, 2012
<http://www.timkelf.com/Research/ResearchSERS.html>, (retrieved 12 january 2012)
41. Raman, C. V., Krishnan K. S., ‘ A New Type of Secondary Radiation’’, *Nature*, Vol. 121, No. 3048, pp. 501-502, 1928.
42. Landsberg and Mandelstam, ‘‘Über die Lichtzerstreuung in Kristallen’’, *Zeitschrift für Physik*, Vol.50, pp. 769-780, 1928.
43. Yu, A. T., Spectroscopy in Biology: Principles and Applications, John Wiley, New York, 1982.

44. Fleischman, M., Hendra, P. J., McQuillan, A. J., “Raman spectra of pyridine adsorbed at a silver electrode”, *Chem. Phys. Lett.*, Vol. 26, pp.163-166, 1974.
45. Campion A., Kambhampati, P., “Surface-enhance Raman scattering”, *Chem. Soc. Rev.*, Vol. 27, pp. 241-250, 1988.
46. Moskovits, M., “Surface roughness and the enhanced intensity of Raman scattering by molecules absorbed on metals”, *J. Chem. Phys.*, Vol. 69, pp. 1459-1461, 1978.
47. Persson, B. N. J., “On the theory of surface-enhanced Raman scattering”, *Chem. Phys. Lett.*, Vol. 82, pp. 561-565, 1981.
48. Haynes, C., Mcfarland, A. D., Van Duyne, R. P., “Surface-enhanced Raman spectroscopy”, *Anal. Chem.*, Vol., pp. 339A-346A, 2005.
49. Ozbay, E., “Plasmonics: Merging photonics and electronics at nanoscale dimensions”, *Science*, Vol. 311, pp. 189-193, 2006.
50. Atwater, H. A., “The promise of plasmonics”, *Scientific American*, Vol. 296, pp. 56-63, 2007.
51. Maier, S. A., Atwater, H. A. “Plasmonics: Localization and guiding of electromagnetic energy in metal/dielectric structures”, *J. Appl. Phys.*, Vol. 98, e.011101, 2005.
52. Willets, K. A., Van Duyne, R. P., “Localized Surface Plasmon Resonance spectroscopy and sensing”, *Annu. Rev. Phys. Chem*, Vol. 58, pp. 267,297, 2007.
53. Haes, A. J., Van Duyne, R. P., “An unified view of propagating and localized surface plasmon resonance biosensors”, *Anal. Bioanal. Chem.*, Vol. 379, pp. 920-930, 2004.

54. Hao, E., Schatz, G. C., “Localized surface plasmon resonance (LSPR)”, *J. Chem. Phys.*, Vol. 120, 2004, pp. 357–366,
<http://willets.cm.utexas.edu/LSPR.html>
55. Haes, A. J., Haynes, C. L., McFarland, A. D., Schatz, G. C., Van Duyne, R. P. , Zou, S., “Plasmonic Materials for Surface-Enhanced Sensing and Spectroscopy”, *Mrs Bulletin*, Vol. 30, pp. 368-375, 2005.
56. Pettinger, B., Ren, B., Picardi, G., Schuster, R. And Ertl, G., “Nanoscale probing of absorbed species by tip-enhanced Raman spectroscopy”, *Phys. Rev. Lett.*, Vol. 92, e 096101, 2004.
57. Schatz, G. C., and Van Duyne, R.P., 2002. Handbook of Vibrational Spectroscopy, Wiley, New York, MA, Vol.1, Pp. 759.
58. Brockman, J. M., Nelson, B. P. Corn, R. M., “Surface plasmon resonance imaging measurements of ultrathin organic films”, *Ann. Rev. Phys. Chem.*, Vol. 51, pp. 41-63, 2000.
59. Srituravanich, W., Fang, N., Sun, C., Luo, Q., Zhang, X., “Plasmonic nanolithography”, *Nano Lett.*, Vol. 4, pp. 1085-1088, 2004.
60. Sokolov, K., Follen, M., Aaron J., Pavlova, I, Malpica, A., Lotan, R., Rachards Kortum, R. “Real-time Vital optical imaging of precancer using Anti-epidermal growth factor antibodies conjugated to gold nanoparticles”, *Cancer Res.*, Vol. 63., pp. 1999-2004, 2003.
61. Reinhard, B., Sheikholeslami, S., Mastroianni, A., Alivisatos, A. P., Liphardt, J. “Use of plasmon coupling to reveal the Dynamics of DNA bending and cleavage by Single EcorRV Restriction Enzymes”, *Proc. Natl. Acad. Sci. U.S.A.*, Vol. 104, pp. 2667-2672, 2007.

62. Rosi, N.L., Mirkin, C. A., “Nanostructures in Biodiagnostics”, *Chem. Rev.*, Vol. 105, pp. 1547-1562, 2005.
63. El-Sayed, I. H., Huang, X., El-Sayed, M. A., “Selective Laser Photo-Thermal therapy of Epithelial Carcinoma using Anti- EGFR Antibody conjugated Gold nanoparticles”, *Cancer Lett.*, Vol. 239, pp. 129-135, 2006.
64. O’neal, D. P., Hirsch, L. R., Halas, N. J., Payne, J. D., West, J. L., “Photo-thermal Tumor Ablation in mice using near Infrared-Absorbing Nanoparticles”, *Cancer Lett.*, Vol. 209, pp. 171-176, 2004.
65. Chen, S. H., Carroll, D. L., “Synthesis and characterization of truncated triangular Silver nanoplate”, *Nano Lett.*, Vol. 2, pp. 1003-1007, 2002.
66. Sun, Y. G., Xia, Y. N., “Shape-controlled synthesis of gold and Silver nanoparticles”, *Science*, Vol. 298, No. 5601, pp. 2176-2179, 2002.
67. Prucek, R., L. Kvitek, Hrbač, J., “Silver Colloids-Methods of Preparation and utilization”, *Acta Univ. Palacki. Olom. Chemica*, Vol. 43, pp. 7-27, 2004.
68. Abdulin, T. I., Bondar, O. V., Shtyrlin, Yu. G., Kahraman, M., Culha, M., “Pluronic block copolymer-mediated interactions of organic compounds with noble metal nanoparticles for SERS analysis”, *Langmuir*, 2010, 26(7), 5153-5159.
69. Cam, D., Keseroglu, K., Kahraman, M., Sahin, F., Culha, M., “Multiplex identification of bacteria in bacterial mixtures with surface-enhanced Raman scattering”, *J. Raman Spectrosc*, doi: 10.1002/jrs.2475, 2009.
70. On, S. L. W., “Identification methods for campylobacters, helicobacters and related organisms”, *Clin.Microbiol. Rev.*, Vol. 9, pp. 405-422, 1996.

71. Claydon, M. A., Davey, S. N., Edwards-Jones, V., Gordon, D. B., “The rapid identification of intact microorganisms using mass spectrometry”, *Nat. Biotechnol.*, Vol. 14, pp. 1584-1586, 1996.
72. Haag, A. M., Taylor, S. N., Johnston, K. H., Cole, R. B., “Rapid Identification and Speciation of *Haemophilus* Bacteria by Matrix-Assisted Laser Desorption/Ionization Time-of-Flight Mass Spectrometry”, *J. Mass. Spectrom.*, Vol. 33, pp. 750-756, 1998.
73. Kahraman, M., Yazici, M., Sahin, F., Culha, M., “Convective Assembly of Bacteria for Surface-Enhanced Raman Scattering”, *Langmuir*, Vol. 24, pp. 894-901, 2008.
74. Scully, M. O., Kattawar, G. W., Lucht, R. P., Opatrny, T., Pilloff, H., Rebane, A., Sokolov, A. V., Zubairy, M. S., “FAST CARS: Engineering a laser spectroscopic technique for rapid identification of bacterial spores”, *Proc. Natl. Acad. Sci. U S A* 2002, 99, 10994.
75. Maquelin, K., Kirschner, C., Choo-Smith, L.P., Ngo-Thi, N. A., Van Vreeswijk, T., Stammler, M., Endtz, H. P., Bruining, H. A., Naumann, D., Puppels, G. J., “Prospective study of the performance of vibrational spectroscopies for rapid identification of bacterial and fungal pathogens recovered from blood cultures”, *J. Clin. Microbiol.* 2003, 41, 324-329.
76. Naumann, D. “Infrared and NIR Raman Spectroscopy in Medical Microbiology”, *Proceedings of SPIE - The International Society for Optical Engineering*, Vol. 3257, pp. 245-257, 1998.
77. Rosch, P., Harz, M., Schmitt, M., Peschke, K.D., Ronneberger, O., Burkhardt, H., Motzkus, H.W., Lankers, M., Hofer, S., Thiele, H., Popp, J., “Chemotaxonomic identification of single bacteria by micro-Raman spectroscopy: Application to clean-room-relevant biological contaminations”, *Appl. Environ. Microbiol.*, Vol. 71, pp. 1626-1637, 2005.

78. Dalterio, R. A., Beak, M., Nelson, W. H., Britt, D., Sperry, J. F., Purcell, F. J., "The resonance Raman Microprobe Detection of Single bacterial Cells From a Chromobacterial Mixture", *Appl. Spectrosc.*, Vol. 41, pp. 241-244, 1987.
79. Puppels, G. J., De Mul, F. F.M., Otto, C., Greve, J., Robert-Nicoud, M. D., Arndt-Jovin, J., "Studying single living cells and chromosomes by confocal Raman microspectroscopy", *Nature*, Vol. 347, pp. 301-303, 1990.
80. Mandal, M., Kundu, S., Ghosh, S. K., Jana, N. R., Panigrahi, M., Pal, T., "Sniffing a single molecule through SERS using Au coreAg shell bimetallic nanoparticles", *Curr. Sci.* 2004, Vol. 86, pp. 556.
81. Doering, W. E., Nie, S., "Single-molecule and Single nanoparticle SERS: examining the roles of surface active sites and chemical enhancement", *J. Phys. Chem. B*, Vol. 106, pp. 311-317, 2002.
82. Culha, M., Kahraman, M., Cam, D., Sayın, I., Keseroglu, K., "Rapid Identification of Bacteria and Yeast Using Surface-Enhanced Raman Scattering", doi.10.1002, 2009.
83. Culha, M., Adiguzel, A., Yazici, M. M., Kahraman, M., Sahin, F., Gulluce, M., "Characterization of thermophilic bacteria using surface-enhanced Raman Scattering", *Applied Spectroscopy*, Vol. 62, pp. 1226-1232, 2008.
84. Efrima, S., Bronk, B. V., "Silver colloids Impregnating or coating bacteria", *J. Phys. Chem. B*, Vol. 102, pp. 5947-5950, 1998.
85. Zeiri, L., Efrima, "Surface-enhanced Raman spectroscopy of bacteria: the effect of excitation wavelength and chemical modification of the colloidal milieu", *J. Raman Spectrosc.*, Vol. 36, pp. 667-675, 2005.
86. Sengupta, A.; Mujacic, M.; Davis, E. J., "Detection of Bacteria by surface enhanced Raman spectroscopy", *Anal. Bioanal. Chem.*, Vol. 386, pp. 1379, 2006.

87. Jarvis, R. M., Goodacre, R., “Rapid discrimination of bacteria using surface enhanced Raman spectroscopy”, *Anal. Chem.*, Vol. 76, pp. 40-47, 2004.
88. Premasiri, W. R., Moir, D. T., Klempner, M. S., Krieger, N., Jones, G., Ziegler, L. D., “Characterization of the Surface Enhanced Raman Scattering (SERS) of Bacteria”, *J. Phys. Chem. B*, Vol. 109, pp. 312-320, 2005.
89. Holt, R. E.; Cotton, T. M., “*J. Am. Chem. Soc.* 1989, Vol. 111, pp. 2815-2821.
90. Sengupta, A., Laucks, M. L., Davis, E. J., “Surface-enhanced Raman spectroscopy of bacteria and pollen”, *Appl. Spectrosc.*, Vol. 59, pp. 1016-1023, 2005.
91. Jarvis, R. M., Brooker, A., Goodacre, R., “Surface-enhanced Raman spectroscopy for bacterial discrimination utilizing a scanning electron microscope with a Raman spectroscopy interface”, *Anal. Chem.*, Vol. 76, pp. 5198- 5202, 2004.
92. Khan Z., Al-Thabaiti, S. A., Obaid, A. Y., Al-Youbi, A. O., “Preparation and characterization of silver nanoparticles by chemical reduction method”, *Colloids and Surfaces B: Biointerfaces*, Vol. 82, pp. 513–517, 2011.
93. Movasaghi, Z., Rehman, S., Rehman, I. U., “Raman spectroscopy of biological tissues”, *Applied Spectroscopy Reviews*, Vol. 42, pp. 493-541, 2007.
94. Jarvis, R. M., Brooker, A. , Goodacre, R. , “Surface-enhanced Raman scattering for the rapid discrimination of bacteria”, *Faraday Discuss.*, Vol. 132, pp. 281–292, 2006.
95. Park, C., Lee, Y. J., Lee, S. Y., Oh, H. B., Lee, J., “Determination of the intracellular concentrations of metabolites in *Escherichia coli* collected during the exponential and stationary growth phases using liquid chromatography-mass spectrometry”, *Bull Korean Chem. Soc.*, Vol. 32, pp. 524-530, 2011.

96. Rao D., 'Introduction to Biochemical engineering', New Delhi, India: McGraw Hill, 2006. Pp169.
97. Chan, J. W., Taylor, D. S., Zwerdling, T., Lane, S. T., Ihara, K., Huser, T., "Micro-Raman spectroscopy detects individual neoplastic and normal hematopoietic cells", *Biophysical Journal.*, Vol. 90, pp. 648–656, 2006.
98. Shetty, G., Kedall, C., Shepherd, N., Stone, N., Barr, H. "Raman spectroscopy: Evaluation of biochemical changes in carcinogenesis of oesophagus", *British Journal of Cancer*, Vol. 94, pp. 1460–1464, 2006.
99. Hanlon, E. B., Manoharan, R., Koo, T. W., Shafer, K. E., Motz, J. T., Fitzmaurice, M., Kramer, J. R., Itzkan, I., Dasari, R. R., Feld, M. S., "Prospects for in vivo Raman spectroscopy", *Physics in Medicine and Biology*, Vol. 45, pp. 1-59, 2000.
100. Stone, N., Kendall, C., Smith, J., Crow, P., Barr, H., "Raman spectroscopy for identification of epithelial cancers", *Faraday Discussion*, Vol. 126, pp. 141–157, 2004.
101. Krafft, C., Neudert, L., Simat, T., Salzer, R., "Near infrared Raman spectra of human brain lipids", *Spectrochimica Acta, Part A*, Vol. 61, pp. 1529–1535, 2005.
102. Gniadecka, M., Wulf, H. C., Mortensen, N. N., Nielsen, O. F., Christensen, D. H., "Diagnosis of basal cell carcinoma by Raman spectroscopy", *Journal of Raman Spectroscopy*, Vol. 28, pp. 125–129, 1997.
103. Cheng, W. T., Liu, M. T., Liu, H. N., Lin, S. Y., "Micro-Raman spectroscopy used to identify and grade human skin pilomatrixoma", *Microscopy Research and Technique*, Vol. 68, pp. 75-79, 2005.
104. Cronan, E. J., "Phospholipid alterations during growth of *Escherichia coli*", *Journal of bacteriology*, Vol. 95, pp. 2054-2061, 1968.

105. Hud, N. V., Milanovich, F. P., Balhorn, R., “Evidence of Novel Secondary Structure in DNA-Bound Protamine Is Revealed by Raman Spectroscopy”, *Biochemistry*, Vol. 33, pp. 7528-7535, 1994.
106. Deng, H., Bloomfield, V. A., Benevides, J. M., Thomas, Jr, G. J., “Dependence of the Raman Signature of Genomic B-DNA on Nucleotide Base Sequence”, *Biopolymers*, Vol. 50, pp. 656–666, 1999.
107. Farguharson, S., Shende, C., Inscore, F. E., Maksymiuk, P., Gift, A., “Analysis of 5-fluorouracil in saliva using surface-enhanced Raman spectroscopy”, *Journal of Raman Spectroscopy*, Vol. 36, pp. 208–212, 2005.
108. Dukor, R. K., “Vibrational spectroscopy in the detection of cancer”, *Biomedical Applications*, Vol. 5, pp. 3335–3359, 2002.
109. Frank, C. J., McCreedy, R. L., Redd, D. C. B., “Raman spectroscopy of normal and diseased human breast tissues”, *Analytical Chemistry*, Vol. 67, pp. 777–783, 1995.
110. Stone, N., Kendell, C., Shepherd, N., Crow, P., Barr, H., “Near-infrared Raman spectroscopy for the classification of epithelial pre-cancers and cancers”, *Journal of Raman Spectroscopy*, Vol. 33, pp. 564–573, 2002.
111. Malini, R., Venkatakrishma, K., Kurien, J., “Discrimination of normal, inflammatory, premalignant, and malignant oral tissue: A Raman spectroscopy study”, *Biopolymers*, Vol. 81, pp. 179–193, 2006.
112. Binoy, J., Abraham, J. P., Joe, I. H., Jayakumar, V. S., Petit, G. R., Nielsen, O. F., “NIR-FT Raman and FT-IR spectral studies and ab initio calculations of the anti-cancer drug combretastatin-A4”, *Journal of Raman Spectroscopy*, Vol. 35, pp. 939–946, 2004.
113. Liu, T. T., Lin, Y. H., Hung, C. S., Liu, T. J., Chen, Y., Huang, Y. C., Tsai, T. H., Wang, H. H., Wang, D. W., Wang, Y. L., Lin, C. H., “A High Speed Detection

- Platform Based on Surface-Enhanced Raman Scattering for Monitoring Antibiotic-Induced Chemical Changes in Bacteria Cell Wall”, *Plosone*, Vol. 4, e5470, 2009.
114. Stone, N., Kendell, C., Shepherd, N., Crow, P., Barr, H., “Near-infrared Raman spectroscopy for the classification of epithelial pre-cancers and cancers”, *Journal of Raman Spectroscopy*, Vol. 33, pp. 564–573, 2002.
115. Frank, C.J., McCreecy, R.L., Redd, D. C. B., “Raman spectroscopy of normal and diseased human breast tissues”, *Analytical Chemistry*, Vol. 67, pp. 777–783, 1995.
116. Harz, M., Rosch, P., Peschke, K. D., Ronneberger, O., Burkhardt, H., Popp, J., “Micro-Raman spectroscopic identification of bacterial cells of the genus *Staphylococcus* and dependence on their cultivation conditions”, *Analyst*, Vol. 130, pp. 1543–1550, 2005.
117. Neugebauer, U., Schmid, U., Baumann, K., Ziebuhr, W., Kozitskaya, S., Deckert, V., Schmitt, M., Popp, J., “Towards a detailed understanding of bacterial metabolism spectroscopic characterization of *Staphylococcus epidermidis*”, *ChemPhysChem.*, Vol. 8, pp. 124–137, 2007.